

Title: Creb5 establishes the competence for *Prg4* expression in articular cartilage

Authors: Cheng-Hai Zhang¹, Yao Gao¹, Unmesh Jadhav^{2,3}, Han-Hwa Hung⁴, Kristina M Holton⁵, Alan J. Grodzinsky⁴, Ramesh A. Shivdasani^{2,3,6}, Andrew B. Lassar^{1,*}

Affiliations:

1. Department of Biological Chemistry and Molecular Pharmacology
Blavatnik Institute at Harvard Medical School
240 Longwood Ave., Boston, MA. 02115

2. Department of Medical Oncology and Center for Functional Cancer Epigenetics, Dana-Farber
Cancer Institute, Boston, MA 02215, USA

3. Departments of Medicine, Brigham & Women's Hospital and Harvard Medical School, Boston,
MA 02215, USA

4. Department of Biological Engineering
MIT Room NE47-377, 77 Massachusetts Ave, Cambridge, MA 0213

5. Research Computing, Harvard Medical School, 25 Shattuck Street, Boston, MA 02115

6. Harvard Stem Cell Institute, Cambridge, MA 02138, USA

* corresponding author:

tel. 617-432-3831

fax. 617-738-0516

e. mail: andrew_lassar@hms.harvard.edu

Short Title: Creb5 regulates lubricin expression

Key words: Articular cartilage; chondrocytes; Lubricin; *Prg4*, *Creb5*, Synovial joints

Abstract:

A hallmark of cells comprising the superficial zone of articular cartilage is their expression of lubricin, encoded by the *Prg4* gene, that lubricates the joint and protects against the development of arthritis. Here, we identify Creb5 as a transcription factor that is specifically expressed in superficial zone articular chondrocytes and is required for TGF- β and EGFR signaling to induce *Prg4* expression. Notably, forced expression of Creb5 in chondrocytes derived from the deep zone of the articular cartilage confers the competence for TGF- β and EGFR signals to induce *Prg4* expression. Chromatin-IP and ATAC-Seq analyses have revealed that Creb5 directly binds to two *Prg4* promoter-proximal regulatory elements, that display an open chromatin conformation specifically in superficial zone articular chondrocytes; and which work in combination with a more distal regulatory element to drive induction of *Prg4* by TGF- β . Our results indicate that Creb5 is a critical regulator of *Prg4*/lubricin expression in the articular cartilage.

Introduction

Osteoarthritis (OA) affects over 30 million US adults (CDC statistics). Therapy for OA is limited to symptom relief and, in severe cases, joint replacement surgery. Interventions that either arrest or reverse the progression of OA are currently unknown. With an eye towards this goal, we have sought to develop a comprehensive understanding of the regulatory network that regulates the differentiation and maintenance of articular cartilage, which plays a central role in maintaining the low-friction environment of the joint space. A hallmark of cells comprising the articular cartilage is their expression of proteoglycans, such as the protein lubricin, encoded by the *Prg4* gene, that lubricates the joint and protects against the development of OA^{1,2}. *Prg4* is specifically expressed in the superficial-most layer of the articular cartilage, but not by deeper layers of this tissue²⁻⁷. Fate mapping studies have established that *Prg4*-expressing cells in embryonic and early post-natal joints constitute a progenitor pool for all regions of the articular cartilage in the adult⁸⁻¹⁰. These findings are consistent with prior studies indicating that both superficial and deep zones of the articular cartilage (plus other synovial joint tissues) specifically arise from *Gdf5*-expressing cells in the embryo¹¹⁻¹³. In both humans and mice lacking *Prg4*, the surface of the articular cartilage becomes damaged and precocious joint failure occurs^{1,2}. Notably, decreased levels of lubricin have been observed in the synovial fluid following either surgically induced osteoarthritis in sheep¹⁴, in human synovial fluid samples from patients with either osteoarthritis (OA) or rheumatoid arthritis (RA)¹⁵, and in the menisci from OA patients¹⁶. Furthermore, a decrease in *Prg4*/lubricin expression during aging¹⁷ correlates with increasing sensitivity of aged knees to cartilage degradation following knee joint destabilization¹⁸. Most notably, loss of lubricin (in *Prg4*^{-/-} mice) has been noted to result in significantly higher levels of peroxynitrite, superoxide and cleaved Caspase 3¹⁹, which correlates with both increased levels of both whole-joint friction and cellular apoptosis in *Prg4*^{-/-} mice compared with either wild-type or *Prg4*^{+/-} mice²⁰. Indeed, a hallmark of both aging^{21,22} and OA²³ is a loss of cells in the superficial zone of the articular

cartilage. Conversely, if lubricin protein is either injected directly into the synovial fluid ²⁴⁻²⁸ or over-expressed in the knee joint (via transgene or AAV; ^{29,30}) the articular cartilage tissue is protected from degradation following surgically induced joint-destabilization. Taken together, these findings indicate that *Prg4*/lubricin counters the signaling pathways that lead to cartilage destruction and suggest that identifying a means to induce the sustained expression of *Prg4* in the articular cartilage may attenuate the degradation of articular cartilage observed during either aging or osteoarthritis (OA).

While Foxo ³¹, Nfat ³² and Creb1 ³³ transcription factors (TFs) have been found to modulate *Prg4* expression in articular chondrocytes, the TFs that drive either tissue-specific expression of *Prg4* or region-specific expression of this gene in the superficial zone of articular cartilage have not yet been elucidated. In addition, as *Prg4* is expressed in articular chondrocytes but not in growth plate chondrocytes, we speculated that identification of the TFs that control expression of this gene in the superficial zone of articular cartilage may elucidate how these distinct chondrocyte cell fates are regulated. Several signaling pathways, including Wnt ^{11,34,35}, TGF- β ^{36,37} and EGFR ³⁸, have all been found necessary to maintain the expression of *Prg4* in the superficial zone of articular cartilage. Interestingly however, injurious mechanical compression ³⁹, TGF- β 1 exposure ³⁶, and shear stress from fluid flow ³³ can induce *Prg4* expression exclusively in explants taken from the superficial zone of bovine articular cartilage, and not in explants from middle or deep zones. This highly restricted induction implies that superficial zone cells either secrete additional necessary signals or uniquely express a TF(s) that responds to the inductive signals. Here, we identify Creb5 as a TF that is specifically expressed in both bovine and human superficial zone articular cartilage and is critically required to activate *Prg4* expression, in response to TGF- β and EGFR signaling.

Results

Creb5, a TF expressed selectively in *Prg4*⁺ chondrocytes

In newborn bovine knee joint cartilage, superficial zone chondrocytes (SZCs) expressing *Prg4*/lubricin are readily distinguished from *Prg4*/lubricin-negative deep zone chondrocytes (DZCs, Fig. 1A). As the profound differences between these two tissues likely have a transcriptional basis, we employed RNA-Seq to identify SZC-specific TF genes. Reflecting their common developmental origin⁸⁻¹⁰, SZCs and DZCs differed by only 320 genes (Supplementary Table 1; false discovery rate, FDR <0.05), including ~67-fold higher *Prg4* mRNA levels in SZCs, as expected, and >15-fold higher levels of other SZC marker genes such as *Vitrin*, *Epha3*, *Wif1*, and *Thbs4* (Supplementary Table 1; Fig. 1B). Notably, we found that 29 transcriptional regulators were more highly expressed (at least 2-fold) in SZCs than in DCZs; and only one TF (*Sall1*) was more highly expressed in DZCs (Table 1). The TF gene *Creb5* was the most differentially expressed transcriptional regulator, with ~25-fold higher levels in SZCs than in DZCs (as determined by RNA-Seq; Fig. 1C), approximately equal to the differential expression of *Prg4* in these tissues. Because TGF- β induces *Prg4* specifically in SZCs *in vitro*³⁶ and maintains *Prg4* expression in articular cartilage *in vivo*³⁷, we assessed mRNA levels in SZCs and DZCs cultured with or without TGF- β 2. RT-qPCR revealed ~10-fold induction of *Prg4* by TGF- β 2 only in SZCs, as others have reported³⁶; and a selective 250-fold (*Prg4*) and 40-fold (*Creb5*) greater expression of these transcripts, in response to TGF- β 2, in SZCs versus DZCs (Fig. 2A, compare lanes 2 and 4).

The basic-leucine zipper (bZIP) DNA-binding domain of *Creb5* shares high sequence homology with those of *Atf2*⁴⁰ and *Atf7*⁴¹. In addition, all three TFs carry two conserved N-terminal

Threonine/Proline residues (T59 and T61 in Creb5) that are substrates for the P38, Jun N-terminal (JNK), and extracellular signal-regulated (ERK) kinases (reviewed in ^{42,43}). Consistent with selective *Creb5* mRNA expression in SZCs, a ~65-kDa protein recognized by both Creb5 and phospho-specific Creb5(T61) antibodies is enriched specifically in SZCs (Fig. 2B). Infection of SZCs with lentivirus encoding an shRNA directed against the 3'UTR of *Creb5* substantially diminished these protein levels (Fig. 3C). Of note, phospho-P38 kinase, the active form that can phosphorylate Creb5 on T61, is also more abundant in SZCs than in DZCs (Fig. 2B). Although TGF- β 2 diminished the level of *Creb5* mRNA to ~30% of that in untreated SZCs (Fig. 2A, lanes 1 and 2), this decrease had no appreciable effect on either total or phospho-Creb5 protein levels (Fig. 2B and Fig. 3C). Consistent with the restricted expression of *Creb5* in the superficial zone of bovine articular cartilage, we similarly detected nuclear-localized Creb5 specifically in the lubricin-expressing superficial zone of articular cartilage in adult human femoral head tissue (Fig. 2C)

Prg4 is initially expressed in the articular perichondrium, which encases the epiphyses of the developing long bones (depicted schematically in Fig. 2D); and is subsequently expressed in the superficial-most layer of mature articular cartilage, but not by deeper layers of this tissue ²⁻⁷. We used RNA in situ hybridization to localize *Creb5* transcripts in relation to *Prg4* and *Collagen 2a1* (*Col2a1*) in the elbow joints of newborn mice. Consistent with our findings in bovine articular chondrocytes, we detected *Creb5* transcripts in *Prg4*-expressing cells (Fig. 2E). More specifically, *Creb5* expression was restricted to the articular perichondrium (Fig. 2E, yellow arrow), where *Prg4*⁺ precursor cells are known to generate articular cartilage ⁸⁻¹⁰, and was absent from perichondrial cells adjacent to the nascent metaphyseal growth plates of developing long bones (Fig. 2E, white arrow). While articular chondrocytes express *Col2a1* but not *Matrilin1* (*Matn1*), epiphyseal chondrocytes (which will later undergo endochondral ossification) express both *Matn1*

and *Col2a1*¹⁰. Notably, expression of *Creb5* (and *Prg4*) is restricted to the articular (*Col2a1*⁺/*Matn1*⁻) chondrocytes (Fig. 2E). In developing mouse knees, *Prg4* is expressed in the articular perichondrium, in superficial cells of the prospective meniscus, and in synovial fibroblasts that line the joint cavity^{2,4,44}. *Creb5* immunocytochemistry on newborn mouse knees indicated that *Creb5* protein was specifically expressed and nuclear localized in these very regions (Fig. 2F, yellow arrow designates the articular perichondrium); and was absent from the metaphyseal perichondrium adjacent to the growth plate (Fig. 2F, white arrow). Thus, *Creb5* co-localizes precisely with cells that express *Prg4* in newborn bovine and murine joints, and in adult human articular cartilage.

***Creb5* is necessary for induction of *Prg4* by TGF- β**

To examine the role of *Creb5* in regulating SZC-specific genes in articular chondrocytes, we infected primary bovine SZCs with a control lentivirus (encoding puromycin resistance and carrying a scrambled shRNA) or one engineered to express an shRNA directed against the *Creb5* 3'UTR (Fig. 3A). After selection in puromycin, we cultured the cells for 3 additional days with or without TGF- β 2, in ultra-low attachment dishes to induce a round cell shape, which favors chondrogenic differentiation⁴⁵. The shRNA against the *Creb5* 3'UTR significantly attenuated *Creb5* transcripts (Fig. 3B) and protein (Fig. 3C), and reduced TGF- β 2 induction of *Prg4* by 58% (Fig. 3B; compare lanes 2 and 4). Because shRNAs can have off-target effects⁴⁶, we also infected primary SZCs with lentivirus encoding puromycin-resistance and Cas9 without (control) or with a guide RNA targeting cleavage within the *Creb5* DNA-binding domain (Fig. 3D). After selection in puromycin and culture with or without TGF- β 2, T7 Endonuclease 1 assays⁴⁷ confirmed efficient introduction of indels in the targeted bZIP domain of *Creb5* (Fig. 3E). While 33% of indels (insertion/deletions) induced by CRISPR/Cas9 mutagenesis are predicted to generate mutations within the bZIP domain that still maintain the reading frame for *Creb5*; the remaining 67% will

produce out of frame proteins. However, as the bZIP domain is sufficient for DNA binding by Creb5⁴⁰, either mutation within this domain or production of a truncated out of frame fusion protein would be expected to significantly affect the ability of Creb5 to induce target gene expression. Consistent with the notion that Creb5 DNA binding activity is necessary for TGF- β dependent expression of *Prg4*, TGF- β 2 induction of *Prg4* was reduced by 77% in SZCs containing indels in the *Creb5* bZIP domain (Fig. 3F, compare lanes 2 and 4). Amongst the handful of other SZC-specific genes whose expression we assayed by RT-qPCR, either shRNA-mediated knock-down of *Creb5* or CRISPR/Cas9-generated indels in the bZIP domain of *Creb5* decreased baseline expression of *Epha3*, but not that of *Thbs4* (Figs. 3B and 3F; compare lanes 1 and 3). Interestingly however, in the presence of TGF- β 2, either shRNA-mediated knock-down of *Creb5* or loss of Creb5 DNA interaction decreased the levels of both *Epha3* and *Thbs4* (Figs. 3B and 3F; compare lanes 2 and 4). As TGF- β 2 administration reduced *Creb5* transcript levels but not Creb5 protein levels, it is possible that this treatment both destabilizes pre-existing RNAs in SZCs (such as *Creb5*, *Epha3*, and *Thbs4*) while inducing the expression of *Prg4*, which requires this signal for its expression^{36,37}. Taken together, these findings suggest that Creb5 is necessary to both maintain expression of some SZC-specific genes (i.e., *Epha3* and *Thb4*) in the presence TGF- β signaling; and is essential for TGF- β signals to induce maximal *Prg4* expression.

Creb5 confers competence for *Prg4* expression in DZCs

As both TGF- β ^{36,37} and EGFR³⁸ signaling promote *Prg4* expression in articular cartilage, we asked if these pathways might regulate *Creb5* expression or phosphorylation. Treatment of primary bovine SZCs with TGF- β 2, but not the EGFR agonist TGF- α , reduced *Creb5* mRNA (Fig. 4A, lanes 2 and 3). However, in SZCs the combination of TGF- β 2 and TGF- α synergistically boosted both *Prg4* expression (Fig. 4A, lane 4) and phospho-Creb5 (T61) levels (Fig. 4B). Because

the highly biased expression of *Creb5* in SZCs versus DZCs correlates with the restricted ability of TGF- β to induce *Prg4* expression in superficial zone cells (Fig. 2A), we next asked whether *Creb5* is the key factor distinguishing the competence for *Prg4* induction in SZCs versus DZCs. To this end, we infected DZCs with a pInducer20 lentivirus⁴⁸ engineered to express a doxycycline-inducible *Creb5* cDNA appended with 3 carboxy-terminal hemagglutinin epitope tags (iCreb5-HA). Indeed, treatment of iCreb5-HA infected DZCs with doxycycline, TGF- β 2 and TGF- α boosted *Prg4* expression ~44-fold (Fig. 4C, compare lanes 1 and 7), equal to *Prg4* levels in SZCs treated with the same ligands (Fig. 4C, lane 9). In contrast, iCreb5-DZCs treated with TGF- β 2 and TGF- α failed to activate *Prg4* in the absence of doxycycline (Fig. 5E, lane 6). Thus, forced expression of *Creb5* in DZCs is sufficient to promote the competence for *Prg4* induction by EGFR and TGF- β signals.

In the limbs of newborn mice, expression of both *Creb5* and *Prg4* is robust in articular chondrocytes and is absent from growth plate chondrocytes (Fig. 2F). To begin to determine whether *Creb5* can confer competence for *Prg4* expression in growth plate-like chondrocytes, we infected either a human chondrosarcoma cell line (SW1353) or an immortalized human costal chondrocyte cell line (C-28/I2;⁴⁹) with lentivirus encoding either EGFP or *Creb5*. Notably, forced expression of *Creb5* conferred competence for TGF- β signaling to induce *PRG4* expression in both cell lines (Supplementary Fig. 1). However, in contrast to deep-zone bovine articular chondrocytes, in which the combination of *Creb5* and TGF- β signaling promotes relatively high-level expression of *Prg4* (approximately equal to 75% of *Gapdh* transcript levels), in the human chondrogenic cell lines, the combination of *Creb5* and TGF- β signaling only induced *PRG4* expression to approximately 0.2% of *GAPDH* transcript levels. Taken together, these findings indicate that *Creb5* can confer competence for *Prg4* induction; and suggest that this TF may work

together with other factors in articular chondrocytes to promote high-level expression of *Prg4* in response to TGF- β signals.

Creb5-dependent induction of *Prg4* requires SAPK activity

Because TGF- β 2 and TGF- α synergistically boosted both *Prg4* expression and Creb5 (T61) phosphorylation, we asked whether stress-activated protein kinases (SAPKs) are necessary to induce *Prg4* expression. In SZCs, TGF- β 2 induction of *Prg4* was specifically blocked by SB203580, an inhibitor of p38 kinase, but not by SP600125, a JNK antagonist (Fig. 5A); p38 inhibition altered *Creb5* transcript levels only slightly (Fig. 5A). In iCreb5-DZCs, induction of *Prg4* by TGF- β 2 was partially blocked by both inhibitors, and completely blocked by the combination (Fig. 5B). Thus, SAPKs are necessary to promote *Prg4* expression by either endogenous or exogenous Creb5 in chondrocytes. In addition, the combination of SAPK inhibitors significantly decreased iCreb5 phosphorylation on T61 (Fig. 5C). To clarify whether SAPK phosphorylation of T59 and T61 on Creb5 is necessary for *Prg4* induction, we mutated both these residues to alanine to block phosphorylation, or to aspartic acid to mimic constitutive phosphorylation. The transcriptional activity of a chimeric protein containing the GAL4 DNA binding domain fused to the N-terminus of Creb5 (GAL4-Creb5-(1-128)) was attenuated by simultaneous T59A/T61A mutations, suggesting that phosphorylation of these residues may indeed promote Creb5 transcriptional activity (Supplementary Fig. 2). Interestingly however, a chimeric protein containing full length Creb5 (GAL4-Creb5-(1-508)) drove significantly greater target gene expression than a chimeric protein containing only the N-terminus of Creb5 (GAL4-Creb5-(1-128)), suggesting that regions outside the N-terminus of this protein can also drive transcriptional activation (Supplementary Fig. 2). As anticipated, phospho-Creb5 (T61) antibody failed to recognize both mutant forms of Creb5 (Fig. 5D). Surprisingly however, in response to

TGF- β 2 and/or TGF- α , both mutant iCreb5 forms induced *Prg4* expression to the same level as did wild-type iCreb5 (Fig. 5E). Thus, although SAPKs promote Creb5 T61 phosphorylation, their requirement for *Prg4* induction must depend on phosphorylation either of other proteins, or of Creb5 sites other than T59 and T61.

Identification of *Prg4* regulatory elements

Because the above findings collectively implicate Creb5 as a key regulator of *Prg4* expression, we sought to understand the basis for its crucial role in driving SZC-specific gene expression. Active enhancers and promoters are both marked by relatively accessible regions of chromatin (reviewed in ⁵⁰). To identify genomic sites with differential chromatin access in SZCs and DZCs, we performed the Assay for Transposase-Accessible Chromatin (ATAC-seq, ⁵¹) on nuclei isolated separately from these populations of primary bovine articular chondrocytes. The 907 sites selectively accessible in SZCs were enriched for 4 distinct sequence motifs, including CRE (cAMP response elements; TGACGTCA) and TRE (TPA response elements; TGAGTCA) (Fig. 6A). Both these motifs bind Creb5, either as a homodimer or as a heterodimer with Jun ⁴⁰. In contrast, ATAC-Seq peaks that were selectively accessible in DZCs were most highly enriched for 2 distinct sequence motifs, which serve as binding sites for either Tead or Runx transcription factors (Fig. 6B). Notably, among genes enriched in either SZCs or DZCs which contained transcription start sites located ≤ 25 kb from differentially accessible ATAC sites, we observed a high correlation between chromatin access and zone-specific gene expression (Fig. 6C). This correlation was highest at the *Prg4* locus (Fig. 6C), where 4 distinct regions (E1-E4) were selectively accessible in SZCs (Fig. 7A). Chromatin IP (ChIP) of iCreb5-HA DZCs with HA antibody, followed by PCR analysis of the precipitated DNA, revealed specific occupancy of Creb5 at the two *Prg4* promoter-proximal sites, E1 and E2, and increased binding induced by TGF- β treatment at both candidate *cis*-elements (Fig. 7B). Together, these observations implicate CRE/TRE binding TFs such as

Creb5 in distinguishing the two articular chondrocyte populations. *Atf2*, which is closely related to Creb5, has been found to directly interact with Smad3/4⁵². We observed that Creb5 can similarly co-immunoprecipitate Smad2/3 (Supplementary Figure 3), suggesting that TGF- β signaling may in part increase *Prg4* expression by inducing nuclear translocation of Smad2/3 and consequent interaction with Creb5.

As *Prg4* is a seminal SZC-specific marker, we examined whether SZC-specific sites E1-E4 function as enhancers. To this end, we appended each sequence upstream of the *Prg4* promoter and firefly luciferase cDNA; and assessed the constructs' ability to drive reporter gene expression in primary bovine SZCs or DZCs. While the *Prg4* promoter alone showed little activity, addition of both E1 and E2 upstream elements drove luciferase expression specifically in SZCs, but TGF- β 2 did not add to this effect (Fig. 7C). Thus, E1 and E2 both interact with Creb5-HA (in iCreb5-DZCs) and drive SZC-specific gene activity, but do not respond to TGF- β . In striking contrast, addition of the distal regulatory element E3 to the promoter-proximal E1 and E2 elements robustly induced TGF- β 2 responsive luciferase expression, in both SZCs and DZCs (Fig. 7C). The E4 element alone failed to confer a TGF- β response and did not interfere with the potent activity of E3 (Fig. 7C). Lastly, while treatment of iCreb5-DZCs with doxycycline plus TGF- β 2 weakly induced expression of the E2E1-*Prg4*-luciferase construct, the addition of the E3 element to this reporter strongly enhanced doxycycline-dependent luciferase activity (Fig. 7D). Thus, the E3 element, located 140 kb upstream of the *Prg4* transcription start site, contains an enhancer that responds robustly to TGF- β 2 in both SZ and DZ chondrocytes.

To ask whether the SZC-enriched sites E1-E4 are necessary to drive *Prg4* expression in SZCs, we infected these cells with a lentivirus encoding either only a dead-Cas9-KRAB fusion protein

(dCas9-KRAB) or dCas9-KRAB plus guide RNAs targeting each *cis*-element. Targeting of dCas9-KRAB to putative enhancers recruits the H3K9 methyltransferase SETDB1, hence increasing local H3K9me3 levels and repressing target genes⁵³. Compared to dCas9-KRAB alone, inclusion of guide RNAs against E1, E2, E3 or E4 significantly repressed TGF- β 2 induction of *Prg4* (Fig. 7E). Notably, targeting of E1 with 2 different gRNAs repressed *Prg4* induction to 0.1% of control levels, while targeting of E2, E3, or E4 repressed *Prg4* to 4-36% of control levels, (Fig. 7E). While E1, E2 and E3 all lie upstream of the *Prg4* coding region, E4 is located in an intron of the *Prg4* gene. Thus, it is possible that recruitment of dCas9-KRAB to E4 and consequent deposition of H3K9me3 modification to the *Prg4* gene proper may block progression of RNA polymerase II, and thereby decrease production of *Prg4* mRNA. Taken together, these findings reveal that expression of *Prg4* in SZCs is dependent upon both the proximal *cis*-elements E1 and E2, which bind Creb5, and a distant E3 element, that drives TGF- β responsive gene activity.

Discussion

In this work, we document that *Creb5* is specifically expressed in the superficial zone of the articular cartilage and is necessary for TGF- β signaling to promote *Prg4* expression in superficial zone bovine articular chondrocytes. In developing mouse knees, *Creb5* is expressed in the articular perichondrium, in superficial cells of the prospective meniscus, and in synovial fibroblasts that line the joint cavity; the same tissues that express *Prg4*^{2,4,44}. Thus, *Creb5* is present in the tissues that express *Prg4* in murine, bovine and human joints, and is necessary to maintain competence for *Prg4* expression in superficial zone articular chondrocytes. In addition, when misexpressed in deep zone bovine articular chondrocytes, *Creb5* confers the competence for TGF- β and EGFR signals to induce *Prg4* expression in these cells. The regionalized expression of *Creb5* in the articular cartilage, which is confined to the superficial zone, helps to explain how *Prg4* expression is similarly constrained to this region of the articular cartilage. As nuclear-localized CREB5 is specifically present in the lubricin-expressing superficial zone of articular cartilage in adult human femoral head articular cartilage, it is plausible that this transcription factor may also be necessary to sustain robust lubricin expression in adult human articular cartilage. Loss of *Creb5* function in SZCs decreased the expression of both *Prg4* and other SZC-specific genes (such as *Epha3*). Thus, it seems likely that *Creb5* may play a larger role in maintaining the unique biological properties of the superficial zone of the articular cartilage.

Prior work has indicated that mechanical motion can promote the expression of *Prg4* in articular cartilage via multiple *Creb1*-dependent, fluid flow shear stress-induced signaling pathways³³. In contrast to *Creb5*, whose expression is restricted to the superficial zone of the articular cartilage, *Creb1* transcripts are equally expressed in both superficial and deep zones of this tissue; but at a significantly lower level than *Creb5*. While both *Creb1* and *Creb5* can bind to overlapping binding

sites^{40,54}, their transcriptional activities are modulated by distinct signaling pathways. PKA-mediated phosphorylation of Creb1 (on Ser133) promotes the interaction of this TF with the KIX domain of the co-activator proteins CBP (CREB-binding protein) and/or p300⁵⁵⁻⁵⁷. Both PGE2 and PTHrP signaling pathways (or forskolin treatment), which can all activate PKA, promote *Prg4* expression in cultures of epiphyseal chondrocytes taken from 5-day-old mice³³. Despite its name, *Creb5* is most closely related to the ATF2/7 family⁴⁰, whose transcriptional activity is regulated by SAPK and MAPK signaling pathways (reviewed in^{42,43}). Interestingly, the PKA activator 8-Br-cAMP can induce phosphorylation of ATF2 on T71⁵⁸. As this phosphorylation site is conserved in Creb5, it is possible that PKA signaling may similarly be able to regulate Creb5 activity. Future ChIP-Seq analysis will be necessary to evaluate whether Creb1 and Creb5 share overlapping binding sites on *Prg4* regulatory elements, and whether these TFs work either synergistically or in parallel to activate the expression of *Prg4* in response to differing signaling pathways.

By performing both ATAC-Seq and chromatin-IP (ChIP) for Creb5, we have found that Creb5 directly binds to two *Prg4* promoter-proximal regulatory elements (E1 and E2), which display an open chromatin conformation specifically in superficial zone articular chondrocytes. Interestingly, the *Prg4* promoter-proximal regulatory elements (E1 and E2) which interact with Creb5, can drive superficial zone-specific chondrocyte gene expression, but cannot respond to TGF- β signals. In striking contrast, appending a distal 5' regulatory element (E3), which also displays increased chromatin accessibility in superficial zone articular chondrocytes (but does not directly bind to Creb5), immediately adjacent to the more proximal Creb5 binding elements (in a luciferase reporter construct) drove robust luciferase expression in response to TGF- β 2. Recruitment of a dead-Cas9-KRAB fusion protein to either the *Prg4* promoter-proximal regulatory elements (that bind to Creb5) or to more distal regulatory elements, significantly blunted induction of *Prg4* by TGF- β signals in superficial zone chondrocytes. Our working

hypothesis is that direct interaction of Creb5 with either E1 or E2 alters the chromatin structure of these regulatory elements, such that they can interact with more distal regulatory elements, which in turn drive robust TGF- β -dependent induction of *Prg4* (Fig. 7F). It may be relevant in this regard that Creb5 can bind to DNA as a heterodimer with Jun; and that Jun/Fos (in an AP1 complex) can recruit the SWI/SNF (BAF) chromatin remodeling complex to establish accessible chromatin on targeted enhancer elements⁵⁹. Future studies will be necessary to investigate whether Creb5 can similarly remodel chromatin to establish enhancer accessibility for the interaction of other transcription factors.

Consistent with the restricted expression of Creb5 in the superficial zone of the articular cartilage, we observed that Creb5 binding sites⁴⁰, including CRE (cAMP response elements; TGACGTCA) and TRE (TPA response elements; TGAGTCA), were both enriched in SZC-specific ATAC-Seq peaks. In contrast, binding sites for either Tead or Runx transcription factors were enriched in DZC-specific ATAC-Seq peaks. While it is currently unclear what regulates either the SZC-specific expression of *Creb5* or the occupancy of Tead and Runx transcription factors on DZC-specific accessible regions of chromatin, these findings underscore the differential transcriptional regulation in these two regions of the articular cartilage. Notably, *Prg4* expressing cells in embryonic and neonatal mice have been found to give rise to all regions of the articular cartilage in adult animals, including those in the deep zone of this tissue⁸⁻¹⁰. Thus, the absence of *Creb5* expression in deep zone articular chondrocytes suggests that *Creb5*, which is initially expressed in the precursors of all articular chondrocytes, is somehow down-regulated together with *Prg4*/lubricin in the deep zone of the articular cartilage.

TGF- β ^{36,37}, EGFR³⁸, and Wnt/ β -catenin^{11,34,35} signaling have all been shown to be necessary to maintain expression of *Prg4* in the articular cartilage. Interestingly, we observed that TGF- β and

EGFR signaling pathways augment the ability of either endogenous Creb5 or exogenous iCreb5 to promote expression of *Prg4* in either superficial or deep zone bovine articular chondrocytes, respectively. Binding of Creb5 to *Prg4* promoter-proximal regulatory elements (E1 and E2) was considerably enhanced by TGF- β administration, consistent with our finding that Creb5, like ATF2⁵², can be co-immunoprecipitated with Smad2/3. Thus, TGF- β signaling may increase occupancy of Creb5 on the two *Prg4* promoter-proximal enhancer elements (E1 and E2) by inducing nuclear translocation of Smad2/3 and consequent interaction with Creb5. Future studies will be necessary to determine whether the requirement for Wnt^{11,34,35} and EGFR³⁸ signals to maintain the expression of *Prg4* in articular cartilage is due to modulation of either the expression or activity of Creb5, or of other necessary co-factors. Exogenous Creb5 could drive relatively high-level expression of *Prg4* (approximately equal to 75% of *Gapdh* transcript levels) in deep zone bovine articular chondrocytes treated with TGF- β . In contrast, the combination of *Creb5* and TGF- β signaling only induced *PRG4* expression to approximately 0.2% of *GAPDH* transcript levels in either a human chondrosarcoma cell line (SW1353) or in an immortalized human costal chondrocyte cell line (C-28/12)⁴⁹. Thus, it seems likely that in addition to Creb5, other transcriptional regulators that are unique to articular chondrocytes may play a role in driving high-level level expression of *Prg4*. In addition to Creb5, we found that 28 transcriptional regulators were more highly expressed (at least 2-fold) in SZCs than in DCZs; and only one TF (Sall1) was more highly expressed in DZCs (Table 1). Notably, Nfat binding motifs were significantly enriched in SZC-specific ATAC-Seq peaks, suggesting that members of the Nfat family may cooperate with Creb5 to promote SZC-specific gene expression. Indeed, cartilage-specific deletion of *Nfatc1* in *Nfatc2*-null mice leads to early onset osteoarthritis, and decreased expression of *Prg4*³². Future studies will be necessary to determine whether either Nfat TFs or any of the other SZC-enriched transcriptional regulators play a direct role in driving the expression of either *Prg4* or other SZC-specific genes.

Creb5 shares a high degree of homology with both Atf2 and Atf7 in both its DNA binding domain and its N-terminus, which contains two highly conserved Threonine-Proline sequences (T59 and T61 in Creb5) that are substrates for p38 kinase, JNK, and ERK (reviewed in ^{42,43}). We have found that phosphorylation of Creb5(T61) can be boosted by both EGFR and TGF- β signals in superficial zone chondrocytes and that phosphorylation of Creb5(T61) is blocked in TGF- β treated iCreb5-DZCs by either a p38 inhibitor (SB203580) or a JNK inhibitor (SP600125). In addition, we noted that Stress Activated Protein Kinase (SAPK) function is required to promote *Prg4* expression in either superficial zone chondrocytes (that express endogenous Creb5) or iCreb5-DZCs (programmed to express iCreb5). Substitution of alanine for threonine in the two highly conserved SAPK phosphorylation sites of either Atf2 or Atf7 cripples the activity of the adjacent N-terminal transcriptional activation domain of these proteins ^{60,61} and the biological activity of Atf2 in vivo ⁶². In striking contrast, we found that similar mutations in the SAPK kinase sites of Creb5 (i.e., iCreb5-T59,61A) did not depress the ability of this transcription factor to induce *Prg4* expression in deep zone chondrocytes treated with either an EGFR ligand and/or TGF- β signals. These findings indicate that while Stress Activated Protein Kinases can promote phosphorylation of Creb5 (on T59, T61), induction of *Prg4* expression, by EGFR and TGF- β signals, is dependent upon SAPK-mediated phosphorylation of either other sites in Creb5 or phosphorylation of other substrates. The transcriptional activity of a chimeric protein containing the GAL4 DNA binding domain fused to the N-terminus of Creb5 (GAL4-Creb5-(1-128)) was attenuated by simultaneous T59A/T61A mutations. Thus, it will be interesting to determine whether, in contrast to *Prg4*, the induction of other Creb5 target genes are regulated by phosphorylation of T59 and T61 in Creb5.

Methods

Isolation and culture of bovine articular chondrocytes

The knee joints from 1-2 week old bovine calves were obtained from Research 87 (a local abattoir in Boylston, MA) directly after slaughter. The intact femoropatellar joints was isolated by transecting the femur and mounting the distal segment in a drilling apparatus. The femoropatellar articular cartilage was then exposed by opening the joint capsule, severing the medial, lateral, and cruciate ligaments, and removing the tibia, patella, and surrounding tissue. Four to six cylindrical cores of cartilage and underlying bone, 9.5 mm in diameter and -15 mm deep, were drilled from each facet (medial and lateral) of the femoropatellar groove. During this entire process, the cartilage was kept moist and free of blood by frequent rinsing with sterile PBS supplemented with antibiotics (100 U/ml penicillin and 100 µg/ml streptomycin). Each core was then inserted into a cylindrical sample holder for a sledge microtome (Model 860, American Optical, Buffalo, NY). An initial ~200-300 micron thick slice of superficial zone articular cartilage (SZC) was first harvested via the microtome. The next approximately 4 mm thick slice of middle zone cartilage tissue was then removed from the same core and discarded. Finally, an 800 micron to 1 mm thick slice of deep zone articular cartilage (DZC) was then harvested from the same core. All of the superficial zone slices from a given knee joint were placed in a 50 mL centrifuge tube filled with medium (DMEM with 10 mM HEPES, 0.1 mM nonessential amino acids, and additional 0.4 mM proline, 25 µg/ml ascorbate) and supplemented with 10% fetal bovine serum. Similarly, all deep zone slices from a given joint were placed in a separate tube filled with medium and serum. To isolate chondrocytes from the superficial and deep zone slices, deep zone cartilage shavings were chopped into pieces about 1 mm³. There was no need to chop superficial zone shavings as they are thin enough. Both superficial zone and chopped deep zone cartilage were digested in 10 ml of pronase (1 mg/ml) in DMEM with 1% penicillin & streptomycin for 1 hour. Pronase was replaced by collagenase D (1 mg/ml) in DMEM with 1% penicillin & streptomycin and cartilage tissue was

digested in the incubator at 37 degrees overnight. The next day, the dissociated cells were filtered through a 70 μ m strainer, counted, pelleted for 5 min at 1200rpm and resuspended in DMEM/F12 plus 10% FBS. For lentivirus infection the cells were plated into a 6-well plate (2-3 million cells per well). 24 hours after plating the medium was changed with new DMEM/F12 plus 10% FBS.

RNA-Seq Analysis

Newly isolated bovine superficial zone chondrocytes and deep zone chondrocytes were cultured (in DMEM/F12 plus 10% FBS) for three days prior to performing RNA-Seq analysis. RNA from superficial zone chondrocytes and deep zone chondrocytes were purified using Trizol reagent (Life Technologies). Genomic DNA in RNA samples was removed using TURBO DNA-free™ Kit (Thermo Fisher Scientific, Cat#: AM1907). Total RNA (5 to 10 ng) was purified using the manufacturer's instructions and used to prepare libraries with SMART-Seq v4 Ultra Low Input RNA Kit (Clontech) followed by sequencing on a NextSeq 500 instrument (Illumina) to obtain 75-bp single-end reads. Raw RNA-seq reads were assessed with FastQC 0.11.3 followed by MultiQC 1.2 aggregation⁶³ to determine sequence quality, per-base sequence quality, per-read GC content (~50), and per base N content. Read pairs were aligned to the Bos taurus genome Ensembl build UMD 3.1 version 88 using STAR 2.5.2b⁶⁴ employing a custom index, with read counting for an unstranded library preparation. Counts were normalized using Trimmed Means of M-values (TMM)⁶⁵ as part of the edgeR package^{66,67}, and modelled for biological and gene-wise variation. Differential expression between sample types was determined through the Exact Test in edgeR, with Benjamini-Hochberg⁶⁸ multiple testing correction (FDR) set at < 0.05.

ATAC-Seq Analysis

Newly isolated bovine superficial zone articular chondrocytes and deep zone articular chondrocytes were cultured (in DMEM/F12 plus 10% FBS) for three days prior to performing ATAC-Seq analysis. ATAC-Seq^{51,69} was performed on replicate samples of 8,000 to 35,000

superficial zone chondrocytes or deep zone chondrocytes. Cultured chondrocytes were first digested into single cells using trypsin, and then trypsin was neutralized by serum. Digested single cells were washed twice in ice-cold PBS, resuspended in 50 μ l ice-cold ATAC Lysis Buffer (10 mM Tris-Cl, pH 7.4, 10mM NaCl, 3mM MgCl₂, 0.1% (V/V) Igepal CA-630), and centrifuged at 500 g at 4 °C to isolate nuclear pellets. Nuclear pellets were treated with Nextera Tn5 Transposase (Illumina, FC-121-1030) in a 50 μ l reaction for 30 min at 37 °C. Transposed DNA was immediately isolated using a Qiagen MinElute PCR Purification Kit, and then PCR amplified in a 50 μ l reaction using a common forward primer and different reverse primers with unique barcodes for each sample as per ⁶⁹. After 5 cycles of PCR, 45 μ l of the reaction was kept on ice; while 5 μ l reaction was amplified by RT-qPCR for 20 cycles to determine the cycles required to achieve 1/3 of the maximal RT-qPCR fluorescence intensity. The remaining 45 μ l of the reaction was then amplified by 8 additional cycles to achieve 1/3 of the maximal RT-qPCR fluorescence intensity (as determined above). The amplified DNA was purified using a Qiagen MinElute PCR Purification Kit and primer dimers (<100 bp) were removed using AMPure beads (Beckman Coulter). ATAC-Seq was performed with two biological repeats to ensure the robustness of the data sets. Raw ATAC-Seq reads were aligned to the bovine genome (Bostau 6) using Bowtie2 ⁷⁰. Aligned signals in raw (bam) files were filtered to remove PCR duplicates and reads that aligned to multiple locations. Peaks were identified using MACS v1.4 ⁷¹.

Construction of lentivirus encoding shRNA targeting Creb5

Bovine Creb5 shRNAs targeting the Creb5 3'UTR were designed using Block-iT RNAi designer (Thermo Fisher). The most efficient Creb5 shRNA sequence we identified was: CCG GGC CTT CAA GAA GAG CTG TTG CCT CGA GGC AAC AGC TCT TCT TGA AGG CTT TTT G (targeting sequence is underlined; employed in Fig. 3A-C). Oligos (ordered from Integrated DNA Technologies) were annealed in a 10 μ l reaction (1 μ l Forward oligo (100 μ M), 1 μ l Reverse oligo (100 μ M), 1 μ l T4 ligation buffer (10X), 6.5 μ l nuclease-free H₂O, 0.5 μ l T4 Polynucleotide Kinase

(NEB)) in a PCR machine, programmed to cycle: 37 °C 30 min, 95 °C 5 min, and then ramp down to 25 °C at 5 °C/min. Annealed oligos that are compatible with the sticky ends of EcoRI and AgeI, were diluted (1:100) and cloned into pLKO.1 TRC-Cloning vector (Addgene # 10878) that had been digested with EcoRI and AgeI, and gel purified. Lentiviral vector encoding shRNA targeting bovine *Creb5* (sh*Creb5*) was verified by sequencing (Genewiz). Lentiviral control vector containing a scrambled shRNA (shSCR) was ordered from Addgene (scramble shRNA, Addgene # 1864).

CRISPR/Cas9 targeting the DNA binding domain of *Creb5*

The CRISPR/Cas9 system was used to introduce insertions /deletions (indels) into the *Creb5* DNA binding domain in bovine superficial zone chondrocytes. Briefly, sequence specific sgRNAs that guide Cas9 to the genomic region encoding the *Creb5* DNA binding domain were designed following the instructions located at (<http://crispr.mit.edu/>). The most efficient guide targeting the DNA binding domain of bovine *Creb5* that we identified is: C TGA AGC TGC ATG TTT GTC T (employed in Fig. 3D-F). Oligos (ordered from Integrated DNA Technologies) were annealed in a 10 µl reaction (1 µl Forward oligo (100 µM), 1µl Reverse oligo (100 µM), 1µl T4 ligation buffer (10X), 6.5 µl nuclear-free H₂O, 0.5 µl T4 Polynucleotide Kinase (NEB)) in a PCR machine programmed to cycle: 37 °C 30 min, 95 °C 5 min, and then ramp down to 25 °C at 5 °C/min. The annealed oligos were diluted (1:200) and cloned into lentiCRISPRv2 (Addgene # 52961) using a Golden Gate Assembly strategy (containing: 100 ng circular lentiCRISPRv2, 1 µl diluted oligo, 0.5 µl BsmBI (Thermo Fisher), 1 µl Tango buffer (10X), 0.5 µl DTT (10mM), 0.5 µl ATP (10 mM), 0.5 µl T4 DNA Ligase (NEB), H₂O up to 10 µl) with 20 cycles of: 37 °C 5 min, 21 °C 5 min. The ligation reaction was then treated with PlasmidSafe (Epicentre, Cat#: E3101K) to digest any residual linearized DNA. PlasmidSafe treated plasmid was transformed into Stbl3 competent cells (Thermo Fisher). LentiCRISPR*Creb5*gRNA plasmid containing the *Creb5* gRNA was verified by sequencing (Genewiz). The parental vector, lentiCRISPRv2, was used to generate control

lentivirus.

T7 endonuclease I (T7E1) assay to detect indels in *Creb5*

The T7 endonuclease I (T7E1) assay was used to detect on-target CRISPR/Cas9 induced insertions and deletions (indels) in cultured cells. cDNA derived from mRNA isolated from either lentiCRISPRv2 or lentiCRISPR*Creb5*gRNA infected bovine superficial zone chondrocytes was employed for the T7E1 assay. A 210bp cDNA fragment, which flanks the *Creb5* gRNA cleavage site, was amplified using *Creb5* RT-qPCR primers (Supplementary Table 2) in a 25 μ l PCR reaction (12.5 μ l Q5 High-Fidelity 2X Master Mix, 1.25 μ l Forward Primer, 1.25 μ l Reverse Primer, cDNA, nuclease-free H₂O to a final volume of 25 μ l). After denaturation of the cDNA at 98 °C 30s; the PCR machine was programmed to cycle 35 times at: 98 °C 10 s, 60 °C 15 s, 72 °C 15 s; 72 °C 2 min; 4 °C hold. The PCR product was denatured and annealed in an 18 μ l reaction (15 μ l PCR product, 2 μ l NEB Buffer2 (10X), 1 μ l nuclease-free H₂O) with the following the cycling conditions: 95 °C 10 min; 95-85 °C (ramp rate of - 2°C/sec); 85-25 °C (ramp rate of - 2°C/sec). After denaturing and reannealing the PCR products, T7 endonuclease I (2 μ l) was added, and the mixture was incubated at 37 °C for 60 min. Cleavage of the PCR products by T7 endonuclease was assayed by agarose gel electrophoresis.

Generation of lentivirus encoding either WT or mutant i*Creb5*

Total RNA (containing *Creb5* transcripts) was isolated from bovine superficial zone articular chondrocytes using Trizol reagent (Life Technologies). cDNA was reverse transcribed using the oligo dT reverse transcription kit SuperScript® III First-Strand Synthesis System (Life Technologies, cat. no. 18080051). The bovine *Creb5* open reading frame (508aa; see NM_001319882.1) was predicted by RNA-Seq of bovine superficial zone articular chondrocytes. A 1524 bp cDNA fragment (encoding 508aa) was PCR amplified from bovine superficial zone articular chondrocyte cDNA using the Q5 High-Fidelity 2X Master Mix (NEB, cat. no. M0492S)

and then cloned into the pCR®-Blunt vector (Life Technologies, Cat#: K270020). Using the pCR®-Blunt-bovine Creb5 as a template, a fragment of DNA encoding 3xHA tags was added onto the C-terminus of Creb5 (immediately before the stop codon). HA-tagged Creb5 was then cloned into a Gateway vector (pENTR-Creb5-HA) using the pENTR™/SD/D-TOPO® Cloning Kit (Life Technologies, Cat#: K2420-20). Creb5-HA was then transferred from pENTR-Creb5-HA into the pInducer20 (Addgene # 44012) lentivirus destination vector or into the pLenti CMV Puro DEST (w118-1) vector (Addgene Plasmid #17452) using Gateway LR Clonase (Thermo Fisher, cat. no. 11791020), to generate pInducer20-iCreb-WT or pLenti-Creb5, respectively. pLenti-GFP vector (EX-EGFP-Lv102) was purchased from GeneCopoeia. To generate lentivirus vectors encoding iCreb5 mutants, the DNA sequence encoding T59/T61 sites in pENTR-Creb5-HA was mutated into sequence encoding either T59/T61A or into T59/T61D, respectively, using the Q5® Site-Directed Mutagenesis Kit (NEB, Cat#: E0554S) following the manufacturer's instructions. Creb5 mutants were then cloned into the lentivirus destination vector pInducer20 using Gateway technology.

Lentivirus encoding dCas9-KRAB targeting *Prg4* ATAC-seq peaks

The CRISPR interference (CRISPRi) system was used to study the function of *Prg4* enhancer elements (E1, 2, 3, 4) in bovine superficial zone chondrocytes. Briefly, sequence specific sgRNAs that direct a dead-Cas9-KRAB fusion protein (dCas9-KRAB; ⁵³) to the genomic region of the *Prg4* enhancer elements were designed following the instructions at CHOPCHOP (<http://chopchop.cbu.uib.no/>). Oligos (ordered from Integrated DNA Technologies) were annealed in a 10 µl reaction (1 µl Forward oligo (100 µM), 1µl Reverse oligo (100 µM), 1µl T4 ligation buffer (10X), 6.5 µl nuclear-free H₂O, 0.5 µl T4 Polynucleotide Kinase) in a PCR machine programmed to cycle: 37 °C 30 min, 95 °C 5 min and then ramp down to 25 °C at 5 °C/min. The annealed oligos were diluted (1:200) and cloned into pLV hU6-sgRNA hUbc-dCas9-KRAB-T2a-Puro (encoding dCas9-KRAB; Addgene # 71236) using a Golden Gate Assembly strategy

(containing: 250 ng circular pLV hU6-sgRNA hUbc-dCas9-KRAB-T2a-Puro, 1 μ l diluted oligo, 0.5 μ l BsmBI (Thermo Fisher), 1 μ l Tango buffer (10X), 0.5 μ l DTT (10mM), 0.5 μ l ATP (10 mM), 0.5 μ l T4 DNA Ligase (NEB) , H₂O up to 10 μ l) with 20 cycles of: 37 °C 5 min, 21 °C 5 min. The ligation reaction above was then treated with PlasmidSafe (Epicentre, Cat#: E3101K) to digest any residual linearized DNA. PlasmidSafe treated plasmid was transformed into Stbl3 (Thermo Fisher) competent cells. dCas9-KRAB plasmids containing the various Prg4 enhancer gRNAs were verified by sequencing (Genewiz). The gRNAs targeting the bovine Prg4 enhancer elements are listed in Supplementary Table 5.

Growth and purification of lentivirus

HEK293 cells were used to package lentivirus. HEK293 cells were plated in a 15-cm dish in 25ml of DMEM/F12 (Invitrogen) supplemented with 10% heat-inactivated fetal bovine serum (Invitrogen) and Pen/Strep at 37°C with 5% CO₂. Transfection was performed when the cells were approximately 70–80% confluent. Lentiviral expression plasmid (6 μ g), psPAX2 (4.5 μ g, Addgene #12260), and pMD2.G VSVG (1.5 μ g, Addgene #12259) plasmids were added into a sterile tube containing 500 μ l of Opti-MEM® I (Invitrogen). In a separate tube, 36 μ l of Fugene 6 was diluted into 500 μ l of Opti-MEM I. The diluted Fugene 6 reagent was added drop-wise to the tube containing the DNA solution. The mixture was incubated for 15–25 minutes at room temperature to allow the DNA-Fugene 6 complex to form. The DNA-Fugene 6 complex was directly added to each tissue culture dish of HEK293 cells. After cells were cultured in a CO₂ incubator at 37°C for 12-24 hours, the medium (containing the DNA-Fugene 6 complex) was replaced with 36 ml fresh DMEM/F12 medium supplemented with 10% heat-inactivated fetal bovine serum and penicillin-streptomycin. Cells were again placed in the CO₂ incubator at 37°C; and virus-containing culture medium was collected in sterile capped tubes 48, 72 and 96 hours post-transfection. Cell debris was removed by centrifugation at 500 g for 10 minutes and filtration through nylon low protein-binding filters (SLHP033RS, Millipore). Virus was concentrated by ultracentrifugation

(employing a SW32 rotor at 25K for 2hr and 30min at 4° C) and stored at -80° C.

Infection of chondrocytes with lentivirus and RT-qPCR

Newly isolated bovine superficial zone articular chondrocytes, deep zone articular chondrocytes, SW1353 cells or immortalized human costal chondrocyte cells (C-28/I2; ⁴⁹) were cultured for at least 2-3 days before infection. SW1353 cells were obtained from ATCC (HTB 94). The immortalized human costal chondrocyte cell line (C-28/I2)⁴⁹ was obtained from Dr. Mary Goldring (Hospital for Special Surgery, Weill Cornell Medical College & Weill Cornell Graduate School of Medical Sciences). Ultracentrifuge-concentrated lentivirus was added into DMEM/F12 medium (with 10% FBS) containing 7.5 µg/ml DEAE-Dextran (to increase infection efficiency). 24 hours after infection, medium was replaced with new DMEM/F12 medium (with 10% FBS) containing either 0.8 µg/ml puromycin or 500 µg/ml G418, for selection. After selection (for either 5 days in puromycin or 11 days in G418) the cells were re-plated onto low attachment tissue culture plates (Corning #3471 or #3473) in DMEM/F12 medium (with 10% FBS), without either puromycin or G418. After two to three days culture, RNA was harvested using Trizol reagent and cDNA were synthesized using SuperScript™ III First-Strand Synthesis SuperMix (Invitrogen, Cat#: 11752-050) according manufacture's guidelines. RT-qPCR primers were synthesized by Integrated DNA Technologies. RT-qPCR was performed in an Applied Biosystem 7500 Fast Real-Time PCR Machine. Each experiment was performed with 2-3 biological repeats and each RT-qPCR assay was performed with technical repeats. Prism statistical software (GraphPad) was employed to analyze the data. Statistical analysis was performed using either unpaired or paired t tests. In RT-qPCR experiments, gene expression was normalized to that of either *GAPDH* or *Creb5*, as indicated. Gene expression was analyzed by RT-qPCR, employing at least one primer which was composed of sequences encoded by distinct exons. All RT-qPCR primers are listed in Supplementary Table 2 and Supplementary Table 11.

Construction of GAL4-Creb5 fusion constructs

Using the pCR®-Blunt-bovine Creb5 cDNA as the template, Creb5 (1-128) and Creb5 (1-508) fragments were PCR amplified to lie between a 5' EcoR1 and 3' Xba1 site, using Q5 High-Fidelity 2X Master Mix (NEB, Cat#: M0492S). These amplicons were then cloned into EcoR1/Xba1 cleaved Gal4-HA-HIF1 α (530-652) plasmid (Addgene # 24887), following the removal of the EcoRI-HA-HIF1 α -XbaI fragment from this plasmid. The resulting plasmids were GAL4-Creb5(1-128) and GAL4-Creb5(1-508). GAL4-Creb5(1-128)T59/T61A and GAL4-Creb5(1-128)C18/C23S were generated by inducing point mutations in the GAL4-Creb5(1-128) vector using the Q5® Site-Directed Mutagenesis Kit (NEB, Cat#: E0554S). The control vector GAL4(1-147) was generated by introducing a stop codon immediately after the GAL4(1-147) sequence in the GAL4-Creb5(1-128) vector. All the plasmids were verified by sequencing.

***Prg4*-luciferase constructs and luciferase assays**

Prg4 enhancer/promoter-firefly luciferase constructs were constructed by cloning various *Prg4* regulatory fragments into pGL4.10[*luc2*] vector (Promega). Bovine genomic DNA was extracted from bovine chondrocytes and was used as the template to amplify *Prg4* regulatory regions. A 543 bp fragment encoding the *Prg4* promoter and 5' UTR up to the start codon of *Prg4* was amplified (with flanking BglII-HindIII sites) and cloned into pGL4.10[*luc2*] to generate pGL4.10 *Prg4*-Promoter-luciferase. A 1061 bp fragment encoding *Prg4* Enhancer1, the *Prg4* promoter and the 5' UTR up to the start codon of *Prg4* was amplified (with flanking BglII-HindIII sites) and cloned into pGL4.10[*luc2*] to generate pGL4.10 E1-*Prg4* promoter-luciferase. A 585bp *Prg4* Enhancer2 fragment was amplified (with flanking EcoRV-BglII sites) and cloned into pGL4.10 E1-*Prg4* promoter-luciferase to generate pGL4.10 E2E1-*Prg4* promoter-luciferase. A 802 bp *Prg4* Enhancer3 fragment was amplified (with flanking XhoI-EcoRV sites) and cloned into pGL4.10 E2E1-*Prg4* promoter-luciferase to generate pGL4.10 E3E2E1-*Prg4* promoter-luciferase. A 331bp *Prg4* Enhancer4 fragment was amplified (with flanking NheI-XhoI sites) and cloned into pGL4.10

E3E2E1-*Prg4* promoter-luciferase to generate pGL4.10 E4E3E2E1-*Prg4* promoter-luciferase. High fidelity DNA polymerase (NEB, cat. no. MO492S) was used to generate all the constructs. All the plasmids were verified by sequencing. *Prg4* Promoter and Enhancer 1, 2, 3, 4 sequences are listed in Supplementary Table 4.

Prg4 enhancer/promoter-firefly luciferase reporters were co-transfected together with the pGL4.75 [hRlu/CMV] renilla luciferase reporter (Promega) into either superficial zone chondrocytes, deep zone chondrocytes, or deep zone chondrocytes previously infected with iCreb5WT lentivirus, using Lipofectamine™ LTX (Thermo Fisher, Cat#: 15338030). Twelve hours after transfection, cell culture medium was changed into new medium to remove the Lipofectamine DNA complex. After another twelve hours culture, transfected cells was re-plated into ultra low attachment tissue culture dishes (Corning, Cat#: 3471) for an additional 48 hours culture, in the either the absence or presence of TGF- β and Doxycycline. Cells were harvested and luciferase activity was measured using the Dual-Luciferase® Reporter Assay System (Promega, Cat#: E1960) in a Turner Biosystems Modulus Microplate Reader. Each experiment was performed with 2-3 biological repeats and each luciferase assay was performed with technical repeats. Prism statistical software (GraphPad) was employed to analyze the data. Statistical analysis was performed using either unpaired or paired t tests.

Chromatin IP (ChIP)-PCR Analysis

Bovine deep zone articular chondrocytes infected with iCreb5-HA lentivirus were cultured in ultra low attachment tissue culture dishes (Corning, Cat#: 3471) for 2-3 days in DMEM/F12 supplemented with 10% FBS, in either the absence or presence of Doxycycline or Doxycycline plus TGF- β 2. The chondrocytes were gently centrifuged (200g, 5 minutes), and digested with 0.25% Trypsin-EDTA (Thermo Fisher, Cat#: 25200056) at 37°C for seven minutes (until the tissue was dispersed into single cells). Trypsinization was stopped by adding 10x volume 10% FBS/DMEM.

Digested single cells were fixed in 1% Formaldehyde at room temperature for 20 min with shaking. Formaldehyde was quenched with 125 mM glycine on a shaking platform at room temperature for 10 min. Cells were then washed two times with cold PBS containing protease inhibitor cocktail (Roche) followed by lysis with 500 μ l ChIP sonication buffer (0.5% SDS, 10mM EDTA, 50mM Tris-HCl pH 8.1). Chromatin (from ~5 million cells in 500 μ l ChIP sonication buffer) was sonicated with a Covaris E220 Sonication Machine (PIP=140, CBP=200, DF=5%, Avg Power =7.0, 300s each time, 6 times (Total 30min). Debris was removed by spinning samples 8 minutes at full speed at 4 °C. The chromatin was diluted with ChIP Dilution Buffer (1.1% TritonX-100, 1.2 mM EDTA, 16.7 mM Tris-HCL pH 8.1, 167 mM NaCl) up to 1500ul in 1.5ml eppendorf tube (DNA low bind tube). SDS concentration was adjusted to below 0.2% and TritonX-100 concentration was adjusted to 1%. Five micrograms of antibody (against the antigen of choice) was added to the chromatin and immunoprecipitated overnight at 4 °C. Protein A (15 μ l) and Protein G (15 μ l) beads were washed two times with ChIP Dilution Buffer and then added to the chromatin. The bead-chromatin complex was rotated at 4 °C for 2 hours and then washed two times each with Low Salt Buffer (0.1% SDS, 1% TritonX-100, 2mM EDTA, 20mM Tris-HCl pH 8.1, 150mM NaCl), High Salt Buffer (0.1% SDS, 1% TritonX-100, 2mM EDTA, 20mM Tris-HCl pH 8.1, 500mM NaCl), Lithium Buffer (0.25M LiCl, 1% IGEPAL CA630 (or NP-40), 1% Deoxycholic acid (Sodium Salt), 1mM EDTA, 10mM Tris pH8.1), and finally TE Buffer (10mM Tris-HCl pH8.0, 1mM EDTA). Chromatin-antibody complexes were eluted twice from beads using 100 μ l of Elution Buffer (1% SDS, 0.1M NaHCO₃) by incubation at room temperature for 10 minutes. NaCl was added into the 200 μ l elute to a final 370 mM concentration. Cross-linked chromatin was reversed at 65 °C with shaking overnight followed by adding RNase A (to a final concentration of 0.2 mg/ml) and incubating at 37°C for one hour to digest RNA; and then adding Proteinase K (to a final concentration of 0.1 mg/ml) and incubating at 55 °C for one hour to digest protein. DNA fragments were purified using the PCR-purification kit with Min-Elute Columns (Qiagen) and analyzed using qPCR. In all ChIP-qPCR results, the level of immunoprecipitated DNA was

normalized to that of the input DNA. Antibodies employed for ChIP are listed in Supplementary Table 7. Primers employed for ChIP-qPCR are listed in Supplementary Table 3.

Co-Immunoprecipitation

Bovine deep zone articular chondrocytes were infected with a lentivirus encoding doxycycline-inducible Creb5 (3xHA tags was added onto the C-terminus of Creb5). After selection in G418, six million cells were cultured in low attachment tissue culture plates (Corning #3262) in DMEM/F12 medium (with 10% FBS, 20ng/ml TGF- β 2) in the presence or absence of doxycycline for additional three days. Cells were harvested and suspended in 1.5 ml Mammalian Cell Lysis Buffer (MCLB, 50 mM Tris, pH 7.5, 150 mM NaCl, 0.5 % NP40, 10 mM NaF) with Protease Inhibitors (PIs) Cocktail. The suspension was lysed by gently rocking at 4 °C for 1 hour and spun down at max speed on a table top centrifuge for 20 minutes at 4 °C. In 1.5 ml clear lysate, 100 μ l lysate was kept as input and 25 μ l of monoclonal anti-HA agarose was added into the remaining 1.4 ml sample. The binding was performed on a rocker at 4 °C overnight. After the binding, the agarose was washed with MLCB plus PIs for at least 5 times. The precipitated protein was eluted with NuPAGE LDS sample buffer (Invitrogen) plus NuPAGE Sample Reducing Agent (Invitrogen). The anti-HA agarose immunoprecipitated protein was probed with anti-Smad2/3 antibody by western blot. The input protein was probed with anti-Smad2/3 antibody and anti-HA antibody (Supplementary Table 6).

Western Blots

Bovine superficial zone or deep zone articular chondrocytes were collected and lysed in Lysis Buffer (containing 50mM Tris·HCl, pH 7.4, 1% NP-40, 0.5% Sodium deoxycholate, 1% SDS, 150 mM NaCl, 2mM EDTA, 50mM NaF, protease inhibitor cocktail (Roche)). The cell lysate were incubated on ice for 15 min, and centrifuged at 3000g, at 4 °C to remove cell debris. Protein concentration was measured with a Bio-Rad Protein Assay Kit (BIO-RAD, Cat#: 500-0006). The

protein was denatured at 70 °C for 10 min with LDS Sample Buffer (Invitrogen, Cat#: NP0007) and Sample Reducing Agent (Invitrogen, Cat#: NP0009). General SDS-PAGE processing procedures were followed. The blots were visualized by the enhanced chemiluminescence detection method, employing the Pierce ECL Western Blotting Substrate (Pierce, Cat#: 32106). All primary antibodies used for Western blots are listed in Supplementary Table 6.

Immunohistochemical analysis

Mouse forelimb, hindlimb or human articular cartilage (procured by the National Disease Research Interchange (NDRI)) were dissected and fixed in 4% paraformaldehyde (in PBS) at 4°C overnight, washed with PBS, and incubated in 30% sucrose at 4°C overnight. Tissues were embedded in OCT and frozen sections were cut at 12 µm using a cryostat. Any non-specific binding of primary antibodies was blocked by incubation with PBS containing 0.2% Tween-20 and 5% non-immune goat serum for 1 hour at room temperature. Primary antibody incubation was carried out at 4°C overnight with a rabbit polyclonal antibody to Creb5 (PA5-65593, Thermo Fisher, 1:100), a mouse monoclonal antibody to Prg4 (MABT401, EMD Millipore, 1:50), a rat monoclonal antibody to the HA epitope (11867423001, Sigma, 1:100), or a rabbit polyclonal antibody to Sox9 (AB5535, EMD Millipore, 1:100). After washing in PBST (3 X 15 minutes at room temperature), sections were incubated with Alexa Fluor 488 or 594 conjugated secondary antibodies (Thermo Fisher, 1:250) for 1 hour at room temperature. 4,6-diamidino-2-phenylindole (DAPI; 1µg/ml) was included with the secondary antibodies to stain DNA. Slides were washed in PBST (3 X 15 minutes at room temperature) and mounted under a coverslip with Aqua-mount (13800; Lerner Labs). Images were taken at the Nikon Imaging Center at Harvard Medical School. All antibodies employed for immunohistochemistry are listed in Supplementary Table 8.

In situ hybridization analysis

Digoxigenin (DIG) or fluorescein labeled RNA probes were made using the DIG RNA labeling kit

(Roche, Cat. 11175025910) or fluorescein RNA labeling kit (Roche, cat. no. 11685619910), respectively, per manufacturer's protocol. T7 RNA polymerase (Roche, cat. no. 10881767001), T3 RNA polymerase (Roche, cat. no. 11031171001) or SP6 RNA polymerase (Roche, cat. no. 10810274001) were employed to generate RNA, depending on the particular RNA probe. After DNase I treatment and precipitation, RNA probes were dissolved in 40 µl RNase-free water. Forelimbs or hindlimbs were dissected and fixed in 4% paraformaldehyde (made with DEPC-treated PBS) at 4°C overnight, washed with PBS, and incubated in 30% sucrose (made with DEPC-treated H₂O) at 4°C overnight. Tissues were embedded in OCT and frozen sections were cut at 20 µm using a cryostat. Sections were fixed again with 4% paraformaldehyde (made with DEPC-treated PBS) at room temperature for 5 minutes, washed twice (5 minutes each at room temperature) with PBS containing 0.1% Tween 20 (PBST). The sections were digested with Proteinase K (4 µg/ml in PBS) at room temperature for 8-20 minutes (depending on the RNA probe), washed twice with PBST (5 minutes each) and fixed again with 4% paraformaldehyde (in PBS) at room temperature for 5 minutes. After washing twice with PBST (5 minutes each, at room temperature), sections were acetylated for 10 minutes (at room temperature) in a solution containing 0.25% acetic anhydride and 0.1M triethanolamine (in DEPC-treated H₂O). After washing twice with PBST (5 minutes each, at room temperature) the slides were rinsed in DEPC-treated H₂O, and then air dried. The RNA probe (listed in Supplemental Table 10) was diluted to 100 ng/ml in a 200 µl volume of hybridization solution (as described in ⁷²), and heated at 95 °C for 5 minutes before adding to the slide. Hybridization was performed at 65 °C overnight, and washed according to the protocol outlined in ⁷². After hybridization, washes, and blocking endogenous peroxidase activity, the slides were blocked with 10% heat inactivated goat serum at room temperature for one hour. Anti-DIG-POD antibody (1:100 dilute, Anti-Digoxigenin-POD, Fab fragment, 11207733910, Roche) or Anti-Fluorescein-POD antibody (1:100, Anti-Fluorescein-POD, Fab fragments, 11426346910, Roche) was added and the slides were incubated at 4 °C overnight. After washing in TNT Buffer (100 mM Tris-HCl pH 7.5, 150 mM NaCl, 0.05%

Tween20), the biotin (1:100) amplification reagent (TSA Biotin Kit, NEL749A001KT) or Fluorescein (1:100) amplification reagent (TSA plus Cyanine 3/ Fluorescein System, NEL753001KT) was applied and slides incubated 20 minutes at room temperature to develop the signal. Biotin signal was further detected by Streptavidin Secondary Alexa 594 dyes. Slides were washed in TNT Buffer (3 X 10 minutes at room temperature), rinsed in H₂O, and mounted under a coverslip with Aqua-mount (13800; Lerner Labs).

Statistics and Reproducibility

RNA-Seq was performed with duplicate biological samples. Differential expression of genes between sample types in these data sets was determined through the Exact Test in edgeR, with Benjamini-Hochberg⁶⁸ multiple testing correction (FDR) set at < 0.05. ATAC-Seq was performed with two biological repeats to ensure the robustness of the data sets. RT-qPCR assays and luciferase assays were performed with 2-3 biological repeats and each assay was performed with technical repeats. Prism statistical software (GraphPad) was employed to analyze the data. Statistical analysis was performed using either unpaired or paired t tests.

RNA-Seq and ATAC-Seq primary data

All primary RNA-Seq and ATAC-Seq data sets have been deposited with GEO.

To review GEO accession GSE132379:

Go to <https://www.ncbi.nlm.nih.gov/geo/query/acc.cgi?acc=GSE132379>

Enter token sfgtgoakdvidpaf into the box

References

- 1 Bahabri, S. A. *et al.* The camptodactyly-arthropathy-coxa vara-pericarditis syndrome: clinical features and genetic mapping to human chromosome 1. *Arthritis Rheum* **41**, 730-735, doi:10.1002/1529-0131(199804)41:4<730::AID-ART22>3.0.CO;2-Y (1998).
- 2 Rhee, D. K. *et al.* The secreted glycoprotein lubricin protects cartilage surfaces and inhibits synovial cell overgrowth. *J Clin Invest* **115**, 622-631 (2005).
- 3 Marcelino, J. *et al.* CACP, encoding a secreted proteoglycan, is mutated in camptodactyly-arthropathy-coxa vara-pericarditis syndrome. *Nat Genet* **23**, 319-322, doi:10.1038/15496 (1999).
- 4 Schumacher, B. L., Hughes, C. E., Kuettner, K. E., Caterson, B. & Aydelotte, M. B. Immunodetection and partial cDNA sequence of the proteoglycan, superficial zone protein, synthesized by cells lining synovial joints. *J Orthop Res* **17**, 110-120, doi:10.1002/jor.1100170117 (1999).
- 5 Flannery, C. R. *et al.* Articular cartilage superficial zone protein (SZP) is homologous to megakaryocyte stimulating factor precursor and is a multifunctional proteoglycan with potential growth-promoting, cytoprotective, and lubricating properties in cartilage metabolism. *Biochem Biophys Res Commun* **254**, 535-541, doi:10.1006/bbrc.1998.0104 (1999).
- 6 Jay, G. D., Britt, D. E. & Cha, C. J. Lubricin is a product of megakaryocyte stimulating factor gene expression by human synovial fibroblasts. *J Rheumatol* **27**, 594-600 (2000).
- 7 Jay, G. D., Tantravahi, U., Britt, D. E., Barrach, H. J. & Cha, C. J. Homology of lubricin and superficial zone protein (SZP): products of megakaryocyte stimulating factor (MSF) gene expression by human synovial fibroblasts and articular chondrocytes localized to chromosome 1q25. *J Orthop Res* **19**, 677-687, doi:10.1016/S0736-0266(00)00040-1 (2001).
- 8 Kozhemyakina, E. *et al.* Identification of a Prg4-expressing articular cartilage progenitor cell population in mice. *Arthritis Rheumatol* **67**, 1261-1273, doi:10.1002/art.39030 (2015).
- 9 Li, L. *et al.* Superficial cells are self-renewing chondrocyte progenitors, which form the articular cartilage in juvenile mice. *FASEB J* **31**, 1067-1084, doi:10.1096/fj.201600918R (2017).
- 10 Decker, R. S. *et al.* Cell origin, volume and arrangement are drivers of articular cartilage formation, morphogenesis and response to injury in mouse limbs. *Dev Biol* **426**, 56-68, doi:10.1016/j.ydbio.2017.04.006 (2017).
- 11 Koyama, E. *et al.* A distinct cohort of progenitor cells participates in synovial joint and articular cartilage formation during mouse limb skeletogenesis. *Dev Biol* **316**, 62-73 (2008).
- 12 Rountree, R. B. *et al.* BMP receptor signaling is required for postnatal maintenance of articular cartilage. *PLoS Biol* **2**, e355 (2004).
- 13 Shwartz, Y., Viukov, S., Krief, S. & Zelzer, E. Joint Development Involves a Continuous Influx of Gdf5-Positive Cells. *Cell Rep* **15**, 2577-2587, doi:10.1016/j.celrep.2016.05.055 (2016).
- 14 Young, A. A. *et al.* Proteoglycan 4 downregulation in a sheep meniscectomy model of early osteoarthritis. *Arthritis Res Ther* **8**, R41, doi:10.1186/ar1898 (2006).
- 15 Kosinska, M. K. *et al.* Articular Joint Lubricants during Osteoarthritis and Rheumatoid Arthritis Display Altered Levels and Molecular Species. *PLoS One* **10**, e0125192, doi:10.1371/journal.pone.0125192 (2015).

- 16 Musumeci, G. *et al.* Lubricin expression in human osteoarthritic knee meniscus and synovial fluid: a morphological, immunohistochemical and biochemical study. *Acta Histochem* **116**, 965-972, doi:10.1016/j.acthis.2014.03.011 (2014).
- 17 Musumeci, G. *et al.* Physical activity ameliorates cartilage degeneration in a rat model of aging: a study on lubricin expression. *Scand J Med Sci Sports* **25**, e222-230, doi:10.1111/sms.12290 (2015).
- 18 Huang, H., Skelly, J. D., Ayers, D. C. & Song, J. Age-dependent Changes in the Articular Cartilage and Subchondral Bone of C57BL/6 Mice after Surgical Destabilization of Medial Meniscus. *Sci Rep* **7**, 42294, doi:10.1038/srep42294 (2017).
- 19 Waller, K. A., Zhang, L. X. & Jay, G. D. Friction-Induced Mitochondrial Dysregulation Contributes to Joint Deterioration in Prg4 Knockout Mice. *Int J Mol Sci* **18**, doi:10.3390/ijms18061252 (2017).
- 20 Waller, K. A. *et al.* Role of lubricin and boundary lubrication in the prevention of chondrocyte apoptosis. *Proc Natl Acad Sci U S A* **110**, 5852-5857, doi:10.1073/pnas.1219289110 (2013).
- 21 Stockwell, R. A. The cell density of human articular and costal cartilage. *J Anat* **101**, 753-763 (1967).
- 22 Quintero, M. *et al.* [Cellular aspects of the aging of articular cartilage. I. Condylar cartilage with a normal surface sampled from normal knees]. *Rev Rhum Mal Osteoartic* **51**, 375-379 (1984).
- 23 Pritzker, K. P. *et al.* Osteoarthritis cartilage histopathology: grading and staging. *Osteoarthritis Cartilage* **14**, 13-29, doi:S1063-4584(05)00197-4 [pii] 10.1016/j.joca.2005.07.014 (2006).
- 24 Jay, G. D. *et al.* Prevention of cartilage degeneration and gait asymmetry by lubricin tribosupplementation in the rat following anterior cruciate ligament transection. *Arthritis Rheum* **64**, 1162-1171, doi:10.1002/art.33461 (2012).
- 25 Jay, G. D. *et al.* Prevention of cartilage degeneration and restoration of chondroprotection by lubricin tribosupplementation in the rat following anterior cruciate ligament transection. *Arthritis Rheum* **62**, 2382-2391, doi:10.1002/art.27550 (2010).
- 26 Teeple, E. *et al.* Effects of supplemental intra-articular lubricin and hyaluronic acid on the progression of posttraumatic arthritis in the anterior cruciate ligament-deficient rat knee. *Am J Sports Med* **39**, 164-172, doi:10.1177/0363546510378088 (2011).
- 27 Flannery, C. R. *et al.* Prevention of cartilage degeneration in a rat model of osteoarthritis by intraarticular treatment with recombinant lubricin. *Arthritis Rheum* **60**, 840-847, doi:10.1002/art.24304 (2009).
- 28 Elsaid, K. A. *et al.* The impact of forced joint exercise on lubricin biosynthesis from articular cartilage following ACL transection and intra-articular lubricin's effect in exercised joints following ACL transection. *Osteoarthritis Cartilage* **20**, 940-948, doi:10.1016/j.joca.2012.04.021 (2012).
- 29 Ruan, M. Z. *et al.* Proteoglycan 4 expression protects against the development of osteoarthritis. *Sci Transl Med* **5**, 176ra134, doi:5/176/176ra34 [pii] 10.1126/scitranslmed.3005409 (2013).
- 30 Ruan, M. Z. *et al.* Treatment of osteoarthritis using a helper-dependent adenoviral vector retargeted to chondrocytes. *Mol Ther Methods Clin Dev* **3**, 16008, doi:10.1038/mtm.2016.8 (2016).
- 31 Matsuzaki, T. *et al.* FoxO transcription factors modulate autophagy and proteoglycan 4 in cartilage homeostasis and osteoarthritis. *Sci Transl Med* **10**, doi:10.1126/scitranslmed.aan0746 (2018).
- 32 Greenblatt, M. B. *et al.* NFATc1 and NFATc2 repress spontaneous osteoarthritis. *Proc Natl Acad Sci U S A* **110**, 19914-19919, doi:10.1073/pnas.1320036110 (2013).

- 33 Ogawa, H., Kozhemyakina, E., Hung, H. H., Grodzinsky, A. J. & Lassar, A. B. Mechanical motion promotes expression of Prg4 in articular cartilage via multiple CREB-dependent, fluid flow shear stress-induced signaling pathways. *Genes Dev* **28**, 127-139, doi:10.1101/gad.231969.113 (2014).
- 34 Yasuhara, R. *et al.* Roles of beta-catenin signaling in phenotypic expression and proliferation of articular cartilage superficial zone cells. *Lab Invest* **91**, 1739-1752, doi:labinvest2011144 [pii] 10.1038/labinvest.2011.144 (2011).
- 35 Xuan, F. *et al.* Wnt/beta-catenin signaling contributes to articular cartilage homeostasis through lubricin induction in the superficial zone. *Arthritis Res Ther* **21**, 247, doi:10.1186/s13075-019-2041-5 (2019).
- 36 Niikura, T. & Reddi, A. H. Differential regulation of lubricin/superficial zone protein by transforming growth factor beta/bone morphogenetic protein superfamily members in articular chondrocytes and synoviocytes. *Arthritis Rheum* **56**, 2312-2321, doi:10.1002/art.22659 (2007).
- 37 Wang, Q. *et al.* Cartilage-specific deletion of Alk5 gene results in a progressive Osteoarthritis-like phenotype in mice. *Osteoarthritis Cartilage*, doi:10.1016/j.joca.2017.07.010 (2017).
- 38 Jia, H. *et al.* EGFR signaling is critical for maintaining the superficial layer of articular cartilage and preventing osteoarthritis initiation. *Proc Natl Acad Sci U S A* **113**, 14360-14365, doi:10.1073/pnas.1608938113 (2016).
- 39 Jones, A. R. *et al.* Modulation of lubricin biosynthesis and tissue surface properties following cartilage mechanical injury. *Arthritis Rheum* **60**, 133-142, doi:10.1002/art.24143 (2009).
- 40 Nomura, N. *et al.* Isolation and characterization of a novel member of the gene family encoding the cAMP response element-binding protein CRE-BP1. *J Biol Chem* **268**, 4259-4266 (1993).
- 41 Gaire, M., Chatton, B. & Kedinger, C. Isolation and characterization of two novel, closely related ATF cDNA clones from HeLa cells. *Nucleic Acids Res* **18**, 3467-3473 (1990).
- 42 Watson, G., Ronai, Z. A. & Lau, E. ATF2, a paradigm of the multifaceted regulation of transcription factors in biology and disease. *Pharmacol Res* **119**, 347-357, doi:10.1016/j.phrs.2017.02.004 (2017).
- 43 Diring, J. *et al.* A cytoplasmic negative regulator isoform of ATF7 impairs ATF7 and ATF2 phosphorylation and transcriptional activity. *PLoS One* **6**, e23351, doi:10.1371/journal.pone.0023351 (2011).
- 44 Lee, S. Y., Niikura, T. & Reddi, A. H. Superficial zone protein (lubricin) in the different tissue compartments of the knee joint: modulation by transforming growth factor beta 1 and interleukin-1 beta. *Tissue Eng Part A* **14**, 1799-1808, doi:10.1089/ten.tea.2007.0367 (2008).
- 45 Kumar, D. & Lassar, A. B. The transcriptional activity of Sox9 in chondrocytes is regulated by RhoA signaling and actin polymerization. *Mol Cell Biol* **29**, 4262-4273, doi:MCB.01779-08 [pii] 10.1128/MCB.01779-08 (2009).
- 46 Kaelin, W. G., Jr. Molecular biology. Use and abuse of RNAi to study mammalian gene function. *Science* **337**, 421-422, doi:10.1126/science.1225787 (2012).
- 47 Vouillot, L., Thelie, A. & Pollet, N. Comparison of T7E1 and surveyor mismatch cleavage assays to detect mutations triggered by engineered nucleases. *G3 (Bethesda)* **5**, 407-415, doi:10.1534/g3.114.015834 (2015).
- 48 Meerbrey, K. L. *et al.* The pINDUCER lentiviral toolkit for inducible RNA interference in vitro and in vivo. *Proc Natl Acad Sci U S A* **108**, 3665-3670, doi:10.1073/pnas.1019736108 (2011).

- 49 Goldring, M. B. *et al.* Interleukin-1 beta-modulated gene expression in immortalized human chondrocytes. *J Clin Invest* **94**, 2307-2316, doi:10.1172/JCI117595 (1994).
- 50 Klemm, S. L., Shipony, Z. & Greenleaf, W. J. Chromatin accessibility and the regulatory epigenome. *Nat Rev Genet* **20**, 207-220, doi:10.1038/s41576-018-0089-8 (2019).
- 51 Buenrostro, J. D., Giresi, P. G., Zaba, L. C., Chang, H. Y. & Greenleaf, W. J. Transposition of native chromatin for fast and sensitive epigenomic profiling of open chromatin, DNA-binding proteins and nucleosome position. *Nat Methods* **10**, 1213-1218, doi:10.1038/nmeth.2688 (2013).
- 52 Sano, Y. *et al.* ATF-2 is a common nuclear target of Smad and TAK1 pathways in transforming growth factor-beta signaling. *J Biol Chem* **274**, 8949-8957 (1999).
- 53 Thakore, P. I. *et al.* Highly specific epigenome editing by CRISPR-Cas9 repressors for silencing of distal regulatory elements. *Nat Methods* **12**, 1143-1149, doi:10.1038/nmeth.3630 (2015).
- 54 Gonzalez, G. A. *et al.* A cluster of phosphorylation sites on the cyclic AMP-regulated nuclear factor CREB predicted by its sequence. *Nature* **337**, 749-752, doi:10.1038/337749a0 (1989).
- 55 Chrivia, J. C. *et al.* Phosphorylated CREB binds specifically to the nuclear protein CBP. *Nature* **365**, 855-859, doi:10.1038/365855a0 (1993).
- 56 Arany, Z., Sellers, W. R., Livingston, D. M. & Eckner, R. E1A-associated p300 and CREB-associated CBP belong to a conserved family of coactivators. *Cell* **77**, 799-800, doi:10.1016/0092-8674(94)90127-9 (1994).
- 57 Parker, D. *et al.* Phosphorylation of CREB at Ser-133 induces complex formation with CREB-binding protein via a direct mechanism. *Mol Cell Biol* **16**, 694-703, doi:10.1128/mcb.16.2.694 (1996).
- 58 Liao, H., Hyman, M. C., Baek, A. E., Fukase, K. & Pinsky, D. J. cAMP/CREB-mediated transcriptional regulation of ectonucleoside triphosphate diphosphohydrolase 1 (CD39) expression. *J Biol Chem* **285**, 14791-14805, doi:10.1074/jbc.M110.116905 (2010).
- 59 Vierbuchen, T. *et al.* AP-1 Transcription Factors and the BAF Complex Mediate Signal-Dependent Enhancer Selection. *Mol Cell* **68**, 1067-1082 e1012, doi:10.1016/j.molcel.2017.11.026 (2017).
- 60 Livingstone, C., Patel, G. & Jones, N. ATF-2 contains a phosphorylation-dependent transcriptional activation domain. *EMBO J* **14**, 1785-1797 (1995).
- 61 De Graeve, F. *et al.* Role of the ATF α /JNK2 complex in Jun activation. *Oncogene* **18**, 3491-3500, doi:10.1038/sj.onc.1202723 (1999).
- 62 Breitwieser, W. *et al.* Feedback regulation of p38 activity via ATF2 is essential for survival of embryonic liver cells. *Genes Dev* **21**, 2069-2082, doi:10.1101/gad.430207 (2007).
- 63 Ewels, P., Magnusson, M., Lundin, S. & Kaller, M. MultiQC: summarize analysis results for multiple tools and samples in a single report. *Bioinformatics* **32**, 3047-3048, doi:10.1093/bioinformatics/btw354 (2016).
- 64 Dobin, A. *et al.* STAR: ultrafast universal RNA-seq aligner. *Bioinformatics* **29**, 15-21, doi:10.1093/bioinformatics/bts635 (2013).
- 65 Robinson, M. D. & Oshlack, A. A scaling normalization method for differential expression analysis of RNA-seq data. *Genome Biol* **11**, R25, doi:10.1186/gb-2010-11-3-r25 (2010).
- 66 Robinson, M. D., McCarthy, D. J. & Smyth, G. K. edgeR: a Bioconductor package for differential expression analysis of digital gene expression data. *Bioinformatics* **26**, 139-140, doi:10.1093/bioinformatics/btp616 (2010).
- 67 McCarthy, D. J., Chen, Y. & Smyth, G. K. Differential expression analysis of multifactor RNA-Seq experiments with respect to biological variation. *Nucleic Acids Res* **40**, 4288-4297, doi:10.1093/nar/gks042 (2012).

- 68 Reiner, A., Yekutieli, D. & Benjamini, Y. Identifying differentially expressed genes using false discovery rate controlling procedures. *Bioinformatics* **19**, 368-375, doi:10.1093/bioinformatics/btf877 (2003).
- 69 Buenrostro, J. D., Wu, B., Chang, H. Y. & Greenleaf, W. J. ATAC-seq: A Method for Assaying Chromatin Accessibility Genome-Wide. *Curr Protoc Mol Biol* **109**, 21 29 21-29, doi:10.1002/0471142727.mb2129s109 (2015).
- 70 Langmead, B. & Salzberg, S. L. Fast gapped-read alignment with Bowtie 2. *Nat Methods* **9**, 357-359, doi:10.1038/nmeth.1923 (2012).
- 71 Zhang, Y. *et al.* Model-based analysis of ChIP-Seq (MACS). *Genome Biol* **9**, R137, doi:10.1186/gb-2008-9-9-r137 (2008).
- 72 Shwartz, Y. & Zelzer, E. Nonradioactive in situ hybridization on skeletal tissue sections. *Methods Mol Biol* **1130**, 203-215, doi:10.1007/978-1-62703-989-5_15 (2014).

Acknowledgments: We thank Attila Aszodi, Veronique Lefebvre, Maurizio Pacifici and Cliff Tabin for providing in situ probes; Terence Capellini, April Craft, Vicki Rosen, Matt Warman and Yingzi Yang for their constructive comments on the manuscript; and the Nikon Imaging Center at Harvard Medical School for use of their microscopes and cameras. We thank Mary Goldring for supplying us with human costal chondrocyte cell lines, and Nicholas O’Neill and Shariq Madha for assistance with computational analyses. We acknowledge the use of tissues procured by the National Disease Research Interchange (NDRI) with support from NIH grant U42OD11158. Portions of this research were conducted on the O2 High Performance Compute Cluster, supported by the Research Computing Group, at Harvard Medical School. **Funding:** This work was supported by grants from NIH to A.B.L. (NIAMS: R01AR060735 and R01AR074385) and R. A. S. (NIDDK: R01DK081113 and R01DK082889). Y. G. was supported by a grant from Ean Technology, Co. Ltd.

Author Contributions: C.-H. Z. and A. B. L. designed experiments and wrote the paper. C.-H. Z. and Y. G. conducted experiments and edited the paper. U. J. provided experimental expertise, analyzed RNA-Seq and ATAC-Seq data, and edited the paper. H.-H. H. isolated superficial and deep zone bovine articular cartilage tissue and edited the paper. K. M. H. performed bioinformatics analysis of the RNA-Seq data. A. J. G. and R. A. S. provided experimental expertise and edited the paper.

Competing interests: Authors declare no competing interests.

Data and correspondence: All primary RNA-Seq and ATAC-Seq data sets have been deposited with GEO (GEO accession GSE132379). All data, code, and materials used in the analysis will be made available to any researcher for purposes of reproducing or extending the analysis. Correspondence and material requests should be addressed to A. B. L.

Figure Legends

Fig. 1. Genes that are preferentially expressed in SZCs versus DZCs. (A) Lubricin (brown) is expressed in superficial zone chondrocytes (SZCs; adjacent to red bar) and not in deep zone chondrocytes (DZCs; adjacent to green bar) in bovine articular cartilage. Image of Lubricin immunostaining taken from ⁴⁴. (B) Relative expression of genes that are differentially expressed in superficial zone bovine articular chondrocytes (SZC) versus deep zone bovine articular chondrocytes (DZC). (C) Volcano plot of differentially expressed genes (DEGs) in SZCs and DZCs. Each dot represents one gene. The red dots represent SZC-specific DEGs, the green dots represent DZC-specific DEGs. Note that the TF gene *Creb5* was as differentially expressed as *Prg4*, with ~25-fold higher levels in SZCs than in DZCs.

Fig. 2. *Creb5* is differentially expressed in superficial versus deep zone articular chondrocytes and is specifically expressed in *Prg4*⁺ cells in synovial joints. (A) RT-qPCR analysis of *Prg4* and *Creb5* expression in either SZCs or DZCs cultured in either the absence or presence of TGF- β 2 (20 ng/ml) for 3 days. Gene expression was assayed by RT-qPCR and normalized to *GAPDH*. Lanes 3 and 4 are compared to lanes 1 and 2, respectively. In both this and subsequent figures: *P<0.05, **P<0.01, ***P<0.001, ND (not detected) and ns (non-significant difference) are indicated and error bar indicates standard error of the mean. Similar results have been obtained in 3 independent biological repeats. (B) Western analysis of proteins in SZCs and DZCs. Similar results have been obtained in 2 independent biological repeats. (C) Immunofluorescent staining for CREB5, Lubricin and DAPI (to visualize nuclei) in adult human femoral head articular cartilage. (D) Schematic of *Prg4* expression in a developing long bone cartilage element. (E) Expression of *Collagen2a1* (*Col2*), *Prg4*, *Creb5*, and *Matrilin1* (*Matn1*) in the elbows of Po mice, as detected by fluorescent in situ hybridization. (F) Immunofluorescent staining for *Creb5* and DAPI (to visualize nuclei) in the knee joint of a Po mouse. In (E & F), the

Creb5-expressing articular perichondrium is designated by a yellow arrow; the metaphyseal perichondrium is designated by a white arrow.

Fig. 3. *Creb5* function is necessary for TGF- β -dependent induction of *Prg4* in superficial zone articular chondrocytes. (A-C) shRNA-mediated knock-down of *Creb5* in superficial zone articular chondrocytes. SZCs were infected with a lentivirus encoding either control scrambled shRNA (shSCR, lanes 1 & 2) or sh*Creb5* (lanes 3 & 4), after selection in puromycin, the cells were cultured in either the absence or presence of TGF- β 2 (20 ng/ml) for 3 days. (B) Gene expression was assayed by RT-qPCR and normalized to *GAPDH*. Lanes 3 and 4 are compared to lanes 1 and 2, respectively. Similar results have been obtained in 3 independent biological repeats. (C) Western analysis of proteins in SZCs recognized by antibodies directed against either phospho-*Creb5* (T61), total *Creb5*, or α -tubulin. Similar results have been obtained in 2 independent biological repeats. (D-F) CRISPR-Cas9 mediated mutation of the DNA binding domain of *Creb5* in SZCs. SZCs were infected with a lentivirus encoding Cas9 alone or Cas9 plus a *Creb5* guide RNA (targeting the DNA binding domain), as indicated. After selection in puromycin, the cells were cultured in either the absence or presence of TGF- β 2 (20 ng/ml) for 3 days. (E) T7 Endonuclease 1 assay (which cleaves at mismatches) is displayed for the RT-PCR amplicon encoding the bZIP domain of *Creb5*. (F) Gene expression was assayed by RT-qPCR and normalized to *GAPDH*. Lanes 3 and 4 are compared to lanes 1 and 2, respectively. Similar results have been obtained in 2 independent biological repeats.

Fig. 4. Forced expression of *Creb5* in deep zone articular chondrocytes confers competence for EGFR and TGF- β signals to induce expression of *Prg4*. (A & B) EGFR and TGF- β signals synergistically induce expression of *Prg4* in SZCs. SZCs were treated for 2 days with TGF- β 2 (20 ng/ml) and TGF- α (100 ng/ml), as indicated. (A) Gene expression was assayed

by RT-qPCR and normalized to *GAPDH*. Lanes 2-4 are compared to lane 1. Similar results have been obtained in 3 independent biological repeats. (B) Western analysis of proteins in SZCs. Similar results have been obtained in 2 independent biological repeats. (C) Forced expression of *Creb5* in DZCs promotes synergistic induction of *Prg4* by TGF- α and TGF- β 2. DZCs were infected with a lentivirus encoding doxycycline-inducible *Creb5*. After selection in G418, the cells were cultured in either the absence or presence of doxycycline (1 μ g/ml), TGF- β 2 (20 ng/ml) and TGF- α (100 ng/ml), as indicated for 3 days. Gene expression was assayed in both the i*Creb5*-DZCs (lanes 1-7) and in control SZCs (lanes 8-9) by RT-qPCR and normalized to *GAPDH*. Lanes 2-7 are compared to lanes 1; lane 9 is compared to lane 8. Similar results have been obtained in 3 independent biological repeats.

Fig. 5. *Creb5*-dependent induction of *Prg4* requires SAPK activity, but neither phosphorylation of T59 nor T61 in *Creb5*. (A) TGF- β 2 induced expression of *Prg4* in superficial zone articular chondrocytes is blocked by inhibition of p38 activity. SZCs were cultured in either the absence or presence of TGF- β 2 (20 ng/ml), a p38 inhibitor (SB203580; 10 μ M) or a JNK inhibitor (SP600125; 10 μ M) as indicated for 2 days. Gene expression was assayed by RT-qPCR and normalized to *GAPDH*. Odd and even lanes are compared to lanes 1 and 2, respectively. Similar results have been obtained in 3 independent biological repeats. (B & C) DZCs were infected with a lentivirus encoding doxycycline-inducible *Creb5*-HA. After selection in G418, the cells (i*Creb5*-DZCs) were cultured in either the absence or presence of doxycycline (1 μ g/ml), TGF- β 2 (20 ng/ml), a p38 inhibitor (SB203580; 10 μ M) or a JNK inhibitor (SP600125; 10 μ M), as indicated for 2 days. (B) Gene expression was assayed by RT-qPCR and normalized to *GAPDH*. Lanes 2-3 are compared to lane 1; lanes 4-6 are compared to lane 3. Similar results have been obtained in 3 independent biological repeats. (C) Western analysis of exogenous *Creb5* expression/phosphorylation in i*Creb5*-DZCs. Similar results have been obtained in 2

independent biological repeats. (D & E) DZCs were infected with a lentivirus encoding either iCreb5-WT-HA; iCreb5-T59,61A-HA; or iCreb5-T59,61D-HA. After selection in G418, the cells were cultured in either the absence or presence of doxycycline (1 μ g/ml), TGF- β 2 (20 ng/ml) and TGF- α (100 ng/ml) as indicated for 3 days. (D) Western analysis of iCreb5-WT/mutant expression in iCreb5-DZCs. Similar results have been obtained in 2 independent biological repeats. (E) Gene expression was assayed by RT-qPCR and normalized to *GAPDH*. Relative level of *Prg4* gene expression driven by the iCreb5-mutant was compared to that induced by iCreb5-WT, under each experimental condition. Similar results have been obtained in 3 independent biological repeats.

Fig. 6. Creb5 binding motifs are enriched in SZC-specific ATAC-Seq peaks. (A) Homer motif analysis of ATAC-Seq peaks that are enriched in SZCs versus DZCs indicated that binding sites for Creb5, Nfi, Nfat, and Tbx TFs are enriched in superficial zone-specific ATAC-Seq peaks. (B) Homer motif analysis of ATAC-Seq peaks that are enriched in DZCs versus SZCs indicated that the binding sites for Tead and Runx TFs are enriched in deep zone-specific ATAC-Seq peaks. The frequency of these sequence motifs in zone-specific ATAC-Seq peaks (% of targets) versus their frequency in the genome (% background) is displayed. (C) A high correlation was observed between zone-specific ATAC-Seq sites (located \leq 25 kb from the transcription start site) and zone-specific gene expression in both SZCs and DZCs. This correlation was highest at the *Prg4* locus, where 4 distinct regions (E1-E4) were selectively accessible in SZCs.

Fig. 7. *Prg4* expression is regulated by the combinatorial activity of several regulatory elements. (A) Comparison of RNA-Seq (top tracks) and ATAC-Seq (bottom tracks) surrounding the *Prg4* locus. Signals for either SZCs (red) or DZCs (blue) are displayed. Putative *Prg4* regulatory elements (E1-E4) are indicated. (B) Bovine articular chondrocytes were infected with lentivirus encoding doxycycline-inducible HA-tagged Creb5 (iCreb5-HA). The cells were

cultured in either the absence or presence of doxycycline and TGF- β 2, as indicated. ChIP-qPCR was performed with anti-HA. Creb5-HA occupancy on ATAC-Seq peaks E1-E4 in the *Prg4* locus or in the GAPDH locus are displayed. (C) SZC-enriched ATAC-Seq peaks surrounding the *Prg4* locus work in combination. Either superficial zone (S) or deep zone (D) bovine articular chondrocytes were co-transfected with a firefly luciferase reporter driven by both the *Prg4* promoter plus a combination of enhancers (E1, E2, E3, and E4) surrounding this gene and a CMV-renilla luciferase construct. Relative expression of firefly/renilla luciferase is displayed (E1E2-*Prg4*-promoter construct compared to *Prg4*-promoter-luciferase; all rest compared to E1E2-*Prg4*-promoter luciferase). Similar results have been obtained in 3 independent biological repeats. (D) DZCs were infected with a lentivirus encoding doxycycline-inducible Creb5-HA. After selection in G418, the cells (iCreb5-DZCs) were transfected with *Prg4*- firefly luciferase expression constructs as described above and cultured with TGF- β 2 (20 ng/ml) in either the absence or presence of doxycycline (1 μ g/ml), as indicated for 2 days. Relative expression of firefly/renilla luciferase is displayed. Similar results have been obtained in 2 independent biological repeats. (E) SZCs were infected with lentivirus encoding only dCas9-KRAB or with lentivirus programmed to encode both dCas9-KRAB plus guide RNAs targeting the various SZC-enriched ATAC-seq peaks (2-3 different guides for each ATAC-Seq peak) that surround the *Prg4* locus. After selection in puromycin, the cells were cultured in the presence of TGF- β 2 (20 ng/ml) for 3 days. Gene expression was assayed by RT-qPCR and normalized to *Creb5*. Relative levels of *Prg4* expression in cells expressing dCas9-KRAB plus various guide RNAs (lanes 2-10) are compared to cells expressing only dCas9-KRAB (lane 1). Similar results have been obtained in 3 independent biological repeats. (F) Model for Creb5-dependent induction of *Prg4* expression.

Table 1. Differentially expressed regulators of gene expression

Transcriptional regulators are listed whose expression differed (by indicated LogFC) between SZC and DZC (false discovery rate, FDR <0.05).

Superficial zone enriched regulators of gene expression			
GeneSymbol	Ensembl	logFC	FDR
CREB5	ENSBTAG00000018909	4.626876	4.39E-16
NRIP3	ENSBTAG00000013366	3.322989	6.63E-08
ZFPM2	ENSBTAG00000001649	3.13596	1.33E-09
HOPX	ENSBTAG00000002333	2.985838	1.94E-06
TSHZ2	ENSBTAG00000007917	2.838663	4.46E-06
HOXD3	ENSBTAG00000004835	2.64649	0.001064
DLX3	ENSBTAG00000017409	2.618468	0.000391
NR4A3	ENSBTAG00000001864	2.586009	7.92E-05
HOXD4	ENSBTAG000000039581	2.429548	6.68E-05
TBX5	ENSBTAG00000011384	2.303632	0.000289
PEG3	ENSBTAG00000023338	2.278346	0.000484
TBX18	ENSBTAG00000018161	2.129558	0.041923
ETV5	ENSBTAG00000014915	2.121456	0.004447
TBX15	ENSBTAG00000007767	2.035948	8.00E-05
OSR2	ENSBTAG00000013213	2.016969	0.000634
NR4A2	ENSBTAG00000003650	2.013499	0.001064
HDAC9	ENSBTAG00000003808	1.885373	0.001849
GLI3	ENSBTAG00000010671	1.766052	0.004555
ERG	ENSBTAG00000011001	1.763597	0.000435
NFATC2	ENSBTAG00000018270	1.759048	0.0142
NFKBIZ	ENSBTAG00000010987	1.674727	0.044988
NFIB	ENSBTAG00000027442	1.562924	0.003388
NR4A1	ENSBTAG00000000507	1.53171	0.00366
HR	ENSBTAG00000012036	1.459785	0.013929
DACT1	ENSBTAG00000019421	1.421286	0.02876
ZFP36L1	ENSBTAG00000025434	1.327187	0.031884
TBX4	ENSBTAG00000009968	1.326603	0.023106
ZNF609	ENSBTAG00000015808	1.265181	0.039834
ZNF385C	ENSBTAG000000046162	1.257806	0.038465

Deep zone enriched regulators of gene expression			
GeneSymbol	Ensembl	logFC	FDR
SALL1	ENSBTAG00000008544	-2.62385	0.000294

List of Supplementary Materials:

Supplementary Figures 1-3

Supplementary Tables 1-11

Supplementary Figure Legends

Supplementary Figure 1. Exogenous Creb5 can promote TGF- β dependent induction of Prg4 expression in either a human chondrosarcoma cell line (SW1353) or in an immortalized human costal chondrocyte cell line (C-28/I2; 49). (A) Sw1353 human chondrosarcoma cells (ATCC HTB 94) or (B) C-28/I2 cells were infected with control lentivirus (Lenti-GFP) or Lenti-Creb5. After selection in puromycin, the cells were cultured in either the presence or absence of TGF- β 2 (20 ng/ml) for 3 days in ultra-low attachment plates. Gene expression was assayed by RT-qPCR and normalized to *GAPDH*. Lanes 3 and 4 are compared to lanes 1 and 2, respectively. *P<0.05, **P<0.01, ***P<0.001, ND (not detected) and ns (non-significant difference) are indicated and error bar indicates standard error of the mean. Similar results have been obtained in 3 independent biological repeats.

Supplementary Figure 2. The amino-terminus of Creb5 contains a relatively weak transcriptional activation domain, which requires both SAPK phosphorylation sites and an intact zinc finger domain for maximal activity. (A) Diagrams of GAL4 DNA binding domain fusions with either full length Creb5 (1-508) or with the N-terminus of Creb5 (1-128). Mutations in either the SAPK phosphorylation sites (T59/T61A) or in the zinc finger domain (C18/C23S) are displayed. (B) Expression of various GAL4 DNA binding domain fusions (as

numbered and diagrammed in A) in transfected 293T cells, as detected by a GAL4 western blot. Lane 6 is derived from non-transfected 293T cells. (C) Superficial zone bovine articular chondrocytes were transfected with various GAL4-Creb5 constructs, plus a GAL4-firefly luciferase reporter and a CMV-renilla luciferase reporter; cells were cultured in either the absence or presence of TGF- β 2 (20 ng/ml) and TGF- α (100 ng/ml), as indicated for 3 days. Relative expression of firefly/renilla luciferase is displayed. The relative level of GAL4-firefly luciferase/renilla luciferase, in response to co-transfection of the various GAL4 constructs, were compared across the 4 conditions by paired t test, as indicated. **P<0.01, ***P<0.001 are indicated and error bar indicates SEM.

Supplementary Figure 3. Creb5 can co-immunoprecipitate Smad2/3. Bovine deep zone articular chondrocytes that were programmed to express doxycycline-inducible Creb5 lentivirus (DZC-iCreb5-HA) were cultured in ultra-low attachment dishes in the presence of TGF- β 2 (20 ng/ml) with or without doxycycline (1 μ g/ml) for 3 days. After 3 days culture, cells were collected and co-immunoprecipitation was performed using monoclonal anti-HA agarose. Immunoprecipitated protein was detected using anti-Smad2/3 antibody in western blot. Input protein was detected using anti-Smad2/3 and anti-HA antibody.

Supplementary Tables

Supplementary Table 1. List of genes that are differentially expressed in superficial versus deep zone bovine articular chondrocytes. 320 genes are listed whose expression differed (by indicated LogFC) between SZC and DZC (false discovery rate, FDR <0.05).

GeneSymbol	Ensembl	logFC	FDR
CLCA2	ENSBTAG00000038215	6.413686	1.86E-27
PRG4	ENSBTAG00000011932	6.074861	8.85E-14
PTX3	ENSBTAG00000009012	5.620196	3.45E-08
PGF	ENSBTAG00000013688	5.619841	2.61E-12
EPHA3	ENSBTAG00000006811	5.553086	6.17E-14
MSMP	ENSBTAG00000038777	5.539089	2.46E-23
VIT	ENSBTAG00000024980	5.521829	5.59E-16
PI15	ENSBTAG00000019587	5.520092	3.51E-11
SCARA5	ENSBTAG00000019636	5.44612	9.79E-11
WIF1	ENSBTAG00000014758	5.349408	1.94E-06
RNASE4	ENSBTAG00000019612	5.201033	1.21E-11
SSC5D	ENSBTAG00000030885	5.133126	3.60E-11
EGFLAM	ENSBTAG00000019595	4.988905	7.85E-07
SFRP2	ENSBTAG00000018563	4.980725	2.82E-12
ANG	ENSBTAG00000045492	4.97905	1.12E-10
CYTL1	ENSBTAG00000011163	4.908574	7.86E-16
GDF6	ENSBTAG00000007687	4.828196	5.13E-09
CXCL14	ENSBTAG00000006694	4.772798	2.19E-09
MME	ENSBTAG00000002075	4.635755	2.23E-09
CREB5	ENSBTAG00000018909	4.626876	4.39E-16
CHI3L1	ENSBTAG00000018223	4.575522	3.15E-09
PAPLN	ENSBTAG00000011680	4.486972	1.12E-10
FGL2	ENSBTAG00000009717	4.464958	3.31E-16
TRIM9	ENSBTAG00000010103	4.434986	2.79E-09
CFB	ENSBTAG00000046158	4.403294	2.64E-06
IGSF10	ENSBTAG00000001728	4.400427	1.09E-08
NPNT	ENSBTAG00000006686	4.384392	8.93E-09
ECM1	ENSBTAG00000003806	4.285342	1.23E-07
ABI3BP	ENSBTAG00000026836	4.153228	0.000299
M-SAA3.2	ENSBTAG00000010433	4.101294	3.50E-06
THBS4	ENSBTAG00000012866	4.078526	6.62E-13
NA	ENSBTAG00000046308	4.038614	1.94E-09

NA	ENSBTAG00000048157	3.936513	4.44E-05
SEMA3D	ENSBTAG00000024394	3.850962	1.94E-09
GDF10	ENSBTAG00000001019	3.778762	2.61E-05
THSD4	ENSBTAG00000011644	3.758696	5.03E-14
PDK4	ENSBTAG00000014069	3.756417	6.14E-08
LRRC17	ENSBTAG00000024379	3.741551	4.93E-05
VCAN	ENSBTAG00000014906	3.740006	2.06E-05
TENM2	ENSBTAG00000025071	3.732978	5.20E-08
GAS1	ENSBTAG00000046803	3.690842	1.66E-08
CPZ	ENSBTAG00000014803	3.586632	1.89E-14
MUSTN1	ENSBTAG00000032531	3.571268	5.48E-07
DLK1	ENSBTAG00000037899	3.552924	0.000113
VCAM1	ENSBTAG00000007773	3.520283	4.38E-08
Saa3	ENSBTAG00000022396	3.514325	4.25E-06
ARHGAP24	ENSBTAG00000003959	3.50379	0.000201
CD55	ENSBTAG00000006984	3.486764	0.004158
NA	ENSBTAG00000046324	3.471685	4.80E-06
GFRA2	ENSBTAG00000020665	3.451466	1.53E-05
PLPP3	ENSBTAG00000011640	3.356799	1.21E-10
NRIP3	ENSBTAG00000013366	3.322989	6.63E-08
TNFRSF19	ENSBTAG00000018300	3.302522	0.000161
B3GALT2	ENSBTAG00000019859	3.268	1.24E-05
FAM107A	ENSBTAG00000046763	3.226581	1.57E-06
C1R	ENSBTAG00000008612	3.220342	6.17E-08
NDNF	ENSBTAG00000010634	3.218956	1.58E-07
ZFPM2	ENSBTAG00000001649	3.13596	1.33E-09
FBN2	ENSBTAG00000015307	3.062646	0.001818
EVI2A	ENSBTAG00000009354	3.047301	0.001205
SOD3	ENSBTAG00000013980	3.017837	4.80E-06
KCTD12	ENSBTAG00000001414	2.998146	0.000143
CA9	ENSBTAG00000011420	2.991845	3.07E-06
WNT11	ENSBTAG00000010820	2.986531	1.02E-05
HOPX	ENSBTAG00000002333	2.985838	1.94E-06
FABP4	ENSBTAG00000037526	2.98365	5.50E-06
OLFML2B	ENSBTAG00000034147	2.953301	0.006843
PTGS1	ENSBTAG00000006716	2.926701	6.22E-06
MMP23B	ENSBTAG00000010732	2.899351	0.000143
MGC148692	ENSBTAG00000040398	2.89885	2.30E-10
MTUS2	ENSBTAG00000001094	2.890496	3.13E-06
ITGA9	ENSBTAG00000016566	2.88827	7.75E-09
FAM46C	ENSBTAG00000046509	2.883714	3.59E-05
NEFH	ENSBTAG00000013147	2.872124	0.000143
TNFRSF11B	ENSBTAG00000007423	2.872019	4.60E-10

CACNA1G	ENSBTAG00000009835	2.858374	0.001781
MEST	ENSBTAG00000017223	2.851048	1.65E-06
GLT8D2	ENSBTAG00000000925	2.850532	1.48E-09
RETREG1	ENSBTAG00000016444	2.848553	1.94E-06
TSHZ2	ENSBTAG00000007917	2.838663	4.46E-06
COL5A3	ENSBTAG00000010179	2.824354	0.019754
PDE3B	ENSBTAG00000005218	2.797717	3.50E-06
IGFBP2	ENSBTAG00000005596	2.795852	0.013051
PCSK6	ENSBTAG00000006675	2.763248	1.94E-06
CLEC3B	ENSBTAG00000018331	2.70384	0.000143
CILP	ENSBTAG00000002821	2.701596	1.81E-05
KCNE4	ENSBTAG00000006432	2.690536	1.65E-05
HOXD3	ENSBTAG00000004835	2.64649	0.001064
ELN	ENSBTAG00000019517	2.639989	0.002557
DLX3	ENSBTAG00000017409	2.618468	0.000391
NR4A3	ENSBTAG00000001864	2.586009	7.92E-05
IGFBP5	ENSBTAG00000007062	2.574917	0.008537
LOXL1	ENSBTAG00000009086	2.545622	0.002839
TGM2	ENSBTAG00000016208	2.534316	8.01E-05
TGFBR3	ENSBTAG00000024269	2.528444	0.002433
COL14A1	ENSBTAG00000013369	2.507959	1.84E-05
BMPER	ENSBTAG00000010866	2.481362	1.24E-06
UCP2	ENSBTAG00000003692	2.480991	0.000583
LPAR3	ENSBTAG00000003791	2.474313	0.001818
ADIRF	ENSBTAG000000032774	2.45869	8.37E-05
FXYD1	ENSBTAG00000017816	2.451089	0.000179
PLCG2	ENSBTAG00000002103	2.443748	4.28E-05
CDON	ENSBTAG00000009315	2.434728	1.84E-05
HOXD4	ENSBTAG000000039581	2.429548	6.68E-05
FAT4	ENSBTAG00000003345	2.428817	0.044841
SLCO3A1	ENSBTAG00000001652	2.423582	0.011157
FBLN5	ENSBTAG00000018123	2.377821	0.008227
COLEC12	ENSBTAG00000007705	2.368188	0.000209
REM1	ENSBTAG00000014176	2.359076	0.000661
ANGPTL1	ENSBTAG00000010719	2.356823	0.00016
CYP1B1	ENSBTAG00000010531	2.350998	0.013051
NA	ENSBTAG000000046587	2.348846	0.000986
DSP	ENSBTAG00000015106	2.335661	0.00791
PLXDC1	ENSBTAG00000019347	2.328685	0.020761
COL8A1	ENSBTAG00000013662	2.317868	0.011729
LTBP1	ENSBTAG00000019839	2.310716	0.003831
GSN	ENSBTAG00000019915	2.308596	1.63E-05
TBX5	ENSBTAG00000011384	2.303632	0.000289

TNS1	ENSBTAG00000002485	2.299354	8.75E-05
SULF2	ENSBTAG00000007490	2.296157	2.78E-05
RAPGEF4	ENSBTAG00000020984	2.289535	0.030979
NA	ENSBTAG00000023338	2.278346	0.000484
CRISPLD1	ENSBTAG00000004411	2.269348	0.010677
SEMA6A	ENSBTAG00000020489	2.257947	2.61E-05
ANGPTL4	ENSBTAG00000002473	2.251963	0.001821
TKTL1	ENSBTAG00000020127	2.239015	0.002793
PPP1R14C	ENSBTAG00000026586	2.238447	0.001009
CTSS	ENSBTAG00000017135	2.233163	0.023166
EPYC	ENSBTAG00000007990	2.225344	0.014737
CAPN6	ENSBTAG00000000828	2.222654	0.000299
GSDMD	ENSBTAG00000021474	2.217718	0.003345
LHFPL6	ENSBTAG00000034033	2.212708	0.002196
COL15A1	ENSBTAG00000010082	2.186371	0.007106
ABCA2	ENSBTAG00000047254	2.182861	9.90E-05
KCNMB4	ENSBTAG00000003749	2.182033	0.014288
DCN	ENSBTAG00000003505	2.156495	0.001923
C1S	ENSBTAG00000004840	2.13159	0.000221
GDF5	ENSBTAG00000004429	2.13152	4.60E-05
TBX18	ENSBTAG00000018161	2.129558	0.041923
ADGRG6	ENSBTAG00000020707	2.129292	0.000707
ETV5	ENSBTAG00000014915	2.121456	0.004447
NA	ENSBTAG00000014718	2.112345	0.001504
TMTC2	ENSBTAG00000002888	2.110349	0.035712
MGLL	ENSBTAG00000018248	2.109955	4.78E-05
BOC	ENSBTAG00000013909	2.101934	8.00E-05
SPON2	ENSBTAG00000004261	2.099332	0.00016
RGS7	ENSBTAG00000005410	2.094469	0.02572
CPXM1	ENSBTAG00000011458	2.076185	0.022655
CAPN5	ENSBTAG00000005034	2.075812	0.008355
SYTL1	ENSBTAG00000010253	2.036095	0.042464
TBX15	ENSBTAG00000007767	2.035948	8.00E-05
C1H21ORF91	ENSBTAG00000001395	2.024839	0.025985
ROBO1	ENSBTAG00000009851	2.024379	0.001415
OSR2	ENSBTAG00000013213	2.016969	0.000634
ECM2	ENSBTAG00000024081	2.014009	0.024078
NR4A2	ENSBTAG00000003650	2.013499	0.001064
ANK3	ENSBTAG00000019052	1.999164	0.005438
TWSG1	ENSBTAG00000001805	1.996491	0.00036
HCLS1	ENSBTAG00000001009	1.99617	0.012814
ROBO2	ENSBTAG00000010462	1.995857	1.97E-05
FZD8	ENSBTAG00000015072	1.990916	0.003632

SERPING1	ENSBTAG00000016267	1.985498	0.000971
SCUBE2	ENSBTAG00000020573	1.98541	0.000143
ENPP2	ENSBTAG00000013165	1.968068	7.92E-05
CCDC3	ENSBTAG00000040490	1.957269	0.000593
PTPRK	ENSBTAG00000020829	1.956195	0.019694
MTMR11	ENSBTAG00000012496	1.951643	0.003831
SPON1	ENSBTAG00000009150	1.951236	0.002413
HHIPL2	ENSBTAG00000017561	1.940159	0.01386
NA	ENSBTAG00000005140	1.910258	0.013929
CHD5	ENSBTAG00000040477	1.901525	0.020498
TMEM119	ENSBTAG00000031849	1.90074	0.006279
SCARA3	ENSBTAG00000007657	1.891333	0.001478
HDAC9	ENSBTAG00000003808	1.885373	0.001849
PCOLCE2	ENSBTAG00000016026	1.851407	0.000122
PALMD	ENSBTAG00000017655	1.837583	0.000721
BAMBI	ENSBTAG00000003045	1.81276	0.014737
AOX1	ENSBTAG00000009725	1.812268	0.002481
CLU	ENSBTAG00000005574	1.79616	0.001439
TBC1D2B	ENSBTAG00000012022	1.791442	0.008537
FGD5	ENSBTAG00000006789	1.785963	0.000557
MAN1C1	ENSBTAG00000003069	1.775969	0.03034
CALHM2	ENSBTAG00000009719	1.773359	0.010048
GLI3	ENSBTAG00000010671	1.766052	0.004555
ERG	ENSBTAG00000011001	1.763597	0.000435
NFATC2	ENSBTAG00000018270	1.759048	0.0142
MXRA8	ENSBTAG00000012247	1.755481	0.004935
ANGPTL8	ENSBTAG00000009570	1.702454	0.023797
SEPT_6	ENSBTAG00000004291	1.678712	0.007768
NFKBIZ	ENSBTAG00000010987	1.674727	0.044988
PAPPA	ENSBTAG00000004010	1.674596	0.010584
HHIP	ENSBTAG00000016071	1.667571	0.045071
ISM1	ENSBTAG00000017188	1.649137	0.006867
B2M	ENSBTAG00000012330	1.642082	0.013374
FAM212B	ENSBTAG00000022580	1.640324	0.038465
NID2	ENSBTAG00000021945	1.626185	0.009129
MAMSTR	ENSBTAG00000011617	1.625821	0.033047
PRSS35	ENSBTAG00000026708	1.623109	0.00857
EPHB2	ENSBTAG00000045902	1.617997	0.010454
CACNA1H	ENSBTAG00000026461	1.614478	0.013337
PCOLCE	ENSBTAG00000020528	1.604713	0.025638
B4GALNT3	ENSBTAG00000008553	1.597711	0.031884
FAM105A	ENSBTAG00000000672	1.590045	0.039015
LRIG1	ENSBTAG00000010360	1.58868	0.008227

CDH11	ENSBTAG00000032092	1.574286	0.044841
DUSP1	ENSBTAG00000013863	1.567773	0.008969
NFIB	ENSBTAG00000027442	1.562924	0.003388
GSE1	ENSBTAG00000009918	1.55598	0.023166
GYS1	ENSBTAG00000039958	1.55591	0.015941
SEMA6D	ENSBTAG00000016800	1.552959	0.008227
AXIN2	ENSBTAG00000030162	1.533667	0.012982
NR4A1	ENSBTAG00000000507	1.53171	0.00366
ANTXR1	ENSBTAG00000007808	1.529695	0.031884
PDGFRL	ENSBTAG00000001966	1.523773	0.004616
ATP2B1	ENSBTAG00000009552	1.517672	0.019064
KALRN	ENSBTAG00000002640	1.512667	0.010048
CST3	ENSBTAG00000000598	1.50981	0.017956
SAMD11	ENSBTAG00000008739	1.507139	0.007796
PTN	ENSBTAG00000002317	1.493428	0.020143
LAMA4	ENSBTAG00000008817	1.482668	0.023166
SHROOM4	ENSBTAG00000002996	1.476505	0.040493
PPP3CA	ENSBTAG00000016005	1.473133	0.008862
ADAMTSL3	ENSBTAG00000004645	1.467368	0.012679
HR	ENSBTAG00000012036	1.459785	0.013929
PKD1	ENSBTAG00000020619	1.449335	0.023021
MCC	ENSBTAG00000035858	1.445357	0.020761
LRP11	ENSBTAG00000032007	1.435079	0.019515
DPYD	ENSBTAG00000031358	1.422513	0.019754
DACT1	ENSBTAG00000019421	1.421286	0.02876
CP	ENSBTAG00000012164	1.419365	0.010719
SGCB	ENSBTAG00000014601	1.416265	0.042464
FRY	ENSBTAG00000006771	1.402701	0.046636
EMILIN1	ENSBTAG00000011324	1.402286	0.023678
SULT1A1	ENSBTAG00000008635	1.389287	0.028399
AHDC1	ENSBTAG00000037456	1.380749	0.033955
FGFR2	ENSBTAG00000014064	1.378282	0.049159
ZFP36L1	ENSBTAG00000025434	1.327187	0.031884
TBX4	ENSBTAG00000009968	1.326603	0.023106
LAMA2	ENSBTAG00000010229	1.302299	0.036574
SLC26A2	ENSBTAG00000014615	1.291513	0.026416
ZNF609	ENSBTAG00000015808	1.265181	0.039834
ZNF385C	ENSBTAG00000046162	1.257806	0.038465
VOPP1	ENSBTAG00000012073	1.241714	0.041244
TGFB3	ENSBTAG00000012004	1.22475	0.044841
STK10	ENSBTAG00000017457	1.224316	0.039891
NA	ENSBTAG00000022590	1.216355	0.042029
CRLF3	ENSBTAG00000018381	-1.23176	0.042464

CNN2	ENSBTAG00000020764	-1.29367	0.041923
FAM101A	ENSBTAG00000039688	-1.30988	0.031529
MYO1E	ENSBTAG00000021538	-1.39474	0.017301
FITM2	ENSBTAG00000020030	-1.48332	0.010719
NF2	ENSBTAG00000013153	-1.50528	0.038138
HTATIP2	ENSBTAG00000013419	-1.50609	0.010048
FADS3	ENSBTAG00000015511	-1.51583	0.011157
TMEM98	ENSBTAG00000008913	-1.52744	0.023496
GADD45A	ENSBTAG00000013860	-1.54206	0.014783
APLP1	ENSBTAG00000001151	-1.55549	0.032728
CTH	ENSBTAG00000014791	-1.61777	0.046636
S100A13	ENSBTAG00000021378	-1.62571	0.014737
EFHD1	ENSBTAG00000014596	-1.66013	0.005493
SPNS3	ENSBTAG00000016175	-1.66023	0.03659
TMCC1	ENSBTAG00000006614	-1.6885	0.003044
CTGF	ENSBTAG00000006367	-1.69483	0.038465
MYH14	ENSBTAG00000002580	-1.70869	0.013374
KIF26B	ENSBTAG00000012715	-1.71152	0.019064
AS3MT	ENSBTAG000000036127	-1.71852	0.019064
NA	ENSBTAG00000007662	-1.74003	0.009524
GPC1	ENSBTAG00000015996	-1.74042	0.002905
NA	ENSBTAG00000047083	-1.79682	0.018858
VAV3	ENSBTAG000000031575	-1.79983	0.002196
RARRES2	ENSBTAG00000004215	-1.82238	0.019064
COL2A1	ENSBTAG00000013155	-1.84988	0.012621
STEAP1	ENSBTAG00000015749	-1.85296	0.019064
GRID1	ENSBTAG00000019623	-1.85854	0.013917
USP53	ENSBTAG00000010350	-1.86227	0.005155
CHAD	ENSBTAG000000021302	-1.87777	0.013374
WLS	ENSBTAG00000012976	-1.88918	0.000484
NA	ENSBTAG00000003661	-1.9013	0.006201
SHB	ENSBTAG00000014922	-1.93336	0.005482
NXN	ENSBTAG00000000855	-1.94239	0.008817
SMOC2	ENSBTAG00000013176	-1.96012	0.004293
SLC44A2	ENSBTAG00000002628	-1.97077	0.000237
MDFI	ENSBTAG00000019343	-2.00143	0.000729
MATN3	ENSBTAG00000020893	-2.02219	0.001596
RASD2	ENSBTAG00000017116	-2.02543	0.003282
CDO1	ENSBTAG00000017442	-2.03657	0.000179
KCNK5	ENSBTAG00000011112	-2.03877	0.003056
NIPSNAP1	ENSBTAG00000013152	-2.04915	0.00123
ANKRD6	ENSBTAG00000003455	-2.10934	0.001582
NALCN	ENSBTAG000000037786	-2.11317	0.017301

SYTL2	ENSBTAG00000000460	-2.14084	0.028436
ST8SIA5	ENSBTAG00000001770	-2.1495	0.001237
FRZB	ENSBTAG00000010977	-2.25584	0.00967
NA	ENSBTAG00000045588	-2.28104	0.006607
TYRO3	ENSBTAG00000001694	-2.28189	1.15E-05
NA	ENSBTAG00000048058	-2.289	2.04E-05
VILL	ENSBTAG00000012963	-2.33324	0.000688
TSPAN5	ENSBTAG00000012343	-2.439	0.000491
GSTM3	ENSBTAG00000001842	-2.44264	0.000385
APOD	ENSBTAG00000023600	-2.45409	8.30E-05
FADS2	ENSBTAG00000015505	-2.55679	4.66E-05
EFNB2	ENSBTAG00000016991	-2.57766	1.37E-05
SFRP5	ENSBTAG00000018566	-2.59011	6.65E-07
SALL1	ENSBTAG00000008544	-2.62385	0.000294
C28H10ORF10	ENSBTAG00000002670	-2.64637	0.000299
HS3ST3A1	ENSBTAG00000031107	-2.65185	1.33E-05
SPNS2	ENSBTAG00000007429	-2.8501	0.0018
GRIA3	ENSBTAG00000011833	-2.85547	0.000124
CNMD	ENSBTAG00000025502	-2.88117	2.45E-05
SPOCK1	ENSBTAG00000003502	-2.93261	0.000581
F13A1	ENSBTAG00000007268	-3.58639	1.37E-05
UNC5C	ENSBTAG00000002084	-3.69095	5.20E-08
RSPO3	ENSBTAG00000008121	-3.69529	2.99E-07
ARSI	ENSBTAG00000012834	-3.72553	0.000391
MPV17L	ENSBTAG00000047520	-3.85463	2.94E-08
PCDH10	ENSBTAG00000019977	-3.92475	3.03E-12
NA	ENSBTAG00000046848	-3.9775	0.00264
SLC38A4	ENSBTAG00000014197	-4.00316	5.13E-09
LOXL4	ENSBTAG00000020895	-4.10458	0.001344
PAMR1	ENSBTAG00000012630	-4.53733	3.51E-19

Supplementary Table 2 : RT-qPCR Primers to amplify bovine cDNA

Gene	Forward	Reverse
<i>Prg4</i>	CTTGATTCAGCAAGCTTCTTCTC	ACAGGAAAGCTCCACAGTGC
<i>Creb5</i>	AGGCGGCGGAAATTTCTG	CATGGCTGTTATGGGGCA
<i>EphA3</i>	GCTGATGCTAGACTGCTG	CGGAAGGTAGTAATGTCTG
<i>Thbs4</i>	ACACCAGTGACCAGGTCAGGCT	GGAGAAGCAGAACACGCCGA
<i>Gapdh</i>	TGGTGAAGGTCGGAGTGAAC	TGTAGACCATGTAGTGAAGGTCA

Supplementary Table 3 : ChIP-PCR Primers

	Forward	Reverse
<i>Prg4</i> Enhancer1	AAAAACACTCTTTGCTGG	AGATGGTAAATTGCTTGG
<i>Prg4</i> Enhancer2	AAGTGAGTTGTCGCTTAAA	AAACCAGTTGAACCATCT
<i>Prg4</i> Enhancer3	AGGTACCACGGCTGTTAC	CAGTGTTTCAGACAGCAG
<i>Prg4</i> Enhancer4	GTTTTCAATTGGAAAGCATT	CACAGCCAAAACAATTATC
<i>GAPDH</i> ATAC PEAK	ACACAGGCGCTCCTGGGAAA	TTCCGCCCTCACGTCCAG

Supplementary Table 4: *Prg4* Promoter and Enhancer E1,E2,E3,E4 sequences

Promoter	TAAAGGTGCTTGAAAAGATTTATAAGGATAGTAGTTGGAGAGTTTAGAAAAGA ATCACATTTATGCAATACACCTGCCGGAGGCTTATGAATTTATATTGAGAGTTA AGAGAATGTTGGAATGATAACTGTAAATTAATTTTACTAAAGCTGGTACTT ATTTTTCCCTTCAATATAGGATTTAAACCTTGTACTTTAAGAACATGCTATAAT TTGAATAGAGTTTTAAGATAAGTCTTTTTTTCTATTTGGGAGATTCTAAAGTATT AAAATGGTCAGTAATGTGGTTGAGATGGTGATTTGATGATTTTTTTTTTCTGT ATAAGATTAAATCTAATGGTCAAGTATTTACAATGAATTAAGGCTGGTTATTTT TAAAAGTCTTGCTTTAAGAATGGGAAAGTTTTTTTTATCATTAAATTGAATTTTG AAATTATTGAAATGCTGTAATACAAGCATAAATTAGTGGTGAGATCCAAGAGGC GTTTCTAATACTTTTATTTTCTTTTCAGCGAGGGCTCAGTACCTGAAAACAGCC
E1	AGAAAACCTTATGCCATAAGCTGAAACTAGATAAAGTTTCAAAAACACTCTTTGC TGGGTTAACTGGAAAAAGAAAAAAAAAAGAAATGATACCAGCATTGACTATTT TAAAGTTGTTGCACTAGTCAAAGCCTGCCAAGCAATTTACCATCTCACAGAACA ATTTGTTCACTTCACTTAGAAATTAGAAGTGTGTTTGGGCCAATAAAGCTAAAT TTGTAGTAGTCATTTTTATTAACGGAAGTGTTTTCCAGATGTTACTTAAAGTCTG GTTGTCTGGGACCTGTTCCAATAAATGAGGAAAGTTTGATTTCATAGGTTGTCA CTGTTGATTCTGTCTAACCTTTGGACTAATTGGTTCATCCTAACATATTTGCTCC GGTATATAAGAGCATTGGACATTGGAGAAATTCACCTCTCCTTTTACGGGTAAG TGTCACAGTTAACTTGCTTCATGGAGTTATATGTTTTCAATTCAATAAGGATTTA TTAAAAGTTTATT
E2	TTCAATTTTCCATTGGAGATACGTTTCTCTCTGTTTTCGCTCCAACCCAGGGCTC ACTCCCTCTGCTTCCCTTCTACCTTGCTTTACTATGCAGAATGCCTGAATGCTGGC CAGCTTTTCCTTTGCTAAGGGCTTATGAAATTCCTATTTCAACCAAGCGGTCTCT TTTGGGAAGGCCACATGGGAGTGCAAAGTGAGTTGTCGCTTAAAAAATAAAT TTTTCCGGATCATTGCATTACACAATCTGTAGTTTCTTGACTTTCTGTGTCAA CTAATTTTTAGATTCAAAGCAGAGCCACAGATGGTTCAACTGGTTTCTCAA AGTTTTAAACAATCCCAACTTTAGTTTTACTGGCATTGCAATAAATTGCTCTGCC TTTTCCCTCTCTGGTATTCCTACCTGCCTTGTAAGTAAAGATAGATGGTTC TGTGTAAGACTGTGTCAACTATTTACGTCTAGATTTATCTTTTTTGGCTTTTTAC TTCTTTTCTCCTTAAGTTCCCCACATTCCTTTTCTACAGGAAGCATGGAAAAGAT AAAGGTGCCAGGAAAGATATTAGTTTTTGGCTGCTGCC

E3	AGGGTATGTCTTGCTTTTCTCTTCCCAGGCATGCTTTTGAAAATCCTCCTGCCTCTCTCTCCTTGACCAACAAGCCCTGTCTGCAGTCATGTTTCTCACTCACAGGAAGTCAGTAATCCCTCAGGGGCTAGGGGTTTACTGTGTGTTCCCTTTCAGAGAGTGGCAAACAACGAATTCATCCTGCAGCAGCGATTGCCAGCTTTGAGCTGCCAGGTTTCCTGGAACAAGTCTGCTCAGTGTGTAATGCACCAGGCAACATCTAGAATCCCTCCTCAGCAGGGAGCATTATATAGGGTGATAGAGCCGACCCATCTTTGAAATGTCTTTTTCTGTTGGTGTTCCTCAGGGTTTTTCAGGGCTCTCTGCTTTTAGAGCCTGGCTCTAAGAGGTACCACGGCTGTTACAGTGATGAGTCATCATGACTCCATGGGAGTGTGGAGGAGACCAAGGATGAGTCAGTAGTCTGTCTGTTTCATTACATCTCATCTTGTTTACATATTCTGCTGTCTGAAACACTGTCTTTTCTGGTTTTGAATAAAGTCTTTGTTCTCTCCCTCCCTTACAGAAACATTGCACTCCGTTTAGGTACCAAGTTGGGGGGGTGCTTGGAAAATGAGATAATGGCCATCGTGAATAGGCTCCACTAATAAGGAGGTAGTTCTGAAACCGAACTCTGGTTGGATCTCACTTTGTTTTCTCTCAGTGGTGACTCCCATGTTACTGTAACATGGTCAAGTGTGCGCTGCCCAAGATTATCCAAAACCTATTTGTAATCTGTCTGAGGGGAATAGGGA
E4	GGAAAATTAATCAGCATAGTGGAGGAACATTTCTTAACTCTTCAATGTTTTATTGGAAAGCATTCCAAAATAATGGAGACAACACCCTTGTAAATAAAATCTCAAGTGCAGAGTTCCTGCAGCTTTTCAGATGGACCTATGAGATGACCTTCTTATTATTATCACTCTGATAATTGTTTTGGCTGTGAGACAAAAAACTAAGAATTTATTTTGGGCAGAGGATGGATCGGGAGGGAAGATGATTAGAGAATGATCAATCATTGAGAGAACCATATTAATAGAGGCAATAGTTTATGCCACCAGGGGCAGGTCAGATTACTTGAG

Supplementary Table 5: Sequence of dCas9-KRAB guide RNAs that target the bovine Prg4 enhancers

E1-1#gRNA	G CTC CGG TAT ATA AGA GCA T
E1-2#gRNA	T CAT CCT AAC ATA TTT GCT C
E2-1#gRNA	G ATT GTG TAA TGC AAT GAT C
E2-2#gRNA	A AGG CAG GTA GGA ATA CCA G
E3-1#gRNA	TTAGTGGAGCCTATTCACGA
E3-2#gRNA	AGACAATTTCAAAGATGGGT
E3-3#gRNA	ACTCCGTTTAGGTACCAAGT
E4-1#gRNA	A TTT TGG GCA GAG GAT GGA T
E4-2#gRNA	GTAATCTGACCTGCCCTGG

Supplementary Table 6: Antibodies employed for Western Blots

Cat. No.	Concentration	Target	Host	Vendor
PA5-65593	1:1000	Creb5	Rabbit	Thermo Fisher
9221S	1:500	p-Creb5	Rabbit	Cell Signaling Technology
9211S	1:1000	p-p38	Rabbit	Cell Signaling Technology
9212S	1:1000	P38	Rabbit	Cell Signaling Technology
T9026	1:1000	α-Tubulin	Mouse	Sigma
ab9110	1:1000	HA	Rabbit	abcam
sc-805	1:1000	HA	Rabbit	Santa cruz biotechnology
A14635	1:1000	Creb5	Rabbit	ABclonal
sc-510	1:500	GAL4	Mouse	Santa cruz biotechnology
8685S	1:1000	Smad2/3	Rabbit	Cell Signaling Technology

Supplementary Table 7: Antibodies employed for either ChIP or co-immunoprecipitation (Co-IP)

Cat. No.	Concentration	Target	Host	Vendor
ab9110	5 μg per ChIP	HA	Rabbit	abcam
ab46540	5 μg per ChIP	IgG	Rabbit	abcam
A2095	25 μl per Co-IP	HA	Mouse	Sigma

Supplementary Table 8: Antibodies employed for immunohistochemistry

Cat. No.	Concentration	Target	Host	Vendor
PA5-65593	1:100	Creb5	Rabbit	Thermo Fisher
MABT401	1:50	Prg4	Mouse	EMD Millipore
11867423001	1:100	HA	Rat	Sigma
AB5535	1:100	Sox9	Rabbit	EMD Millipore
18338S	1:50	Phospho-Smad2 (Ser465/Ser467)	Rabbit	Cell Signaling Technology
A11029	1:250	anti-Mouse IgG; Alexa Fluor 488	Goat	Thermo Fisher
A11037	1:250	anti-Rabbit IgG ; Alexa Fluor 594	Goat	Thermo Fisher
A11006	1:250	anti-Rat IgG;	Goat	Thermo

		Alexa Fluor 488		Fisher
S11227	1:250	Streptavidin, Alexa Fluor™ 594 conjugate		Thermo Fisher

Supplementary Table 9: Growth factors and inhibitors used for chondrocyte culture

	Cat. No.	Concentration	Vendor
TGF-α	239-A-100	100 ng/ml	R&D Systems
TGF-β2	302-B2-010	20 ng/ml	R&D Systems
Doxycycline	D9891-1G	1 μg/ml	Sigma
SB203580	152121-47-6	10 μM	TOCRIS
SP600125	129-56-6	10 μM	TOCRIS

Supplementary Table 10: Target sequence (sense strand) of in situ hybridization probes.

Prg4	AGATTCAGAACAACCTGAAGAAACAACCTCCTGCATCAGAAGATTCTGAT GATTCTAAAACAACCTCTAAAACCACAGAAGCCAACCAAGCACCCAAGCC TACCAAAAAGCCAACCAAGCACCCAAGAAGCCCACCTCTACCAAAAAGC CAAAGACACCAAAAACAAGAAAACCAAAAACCTACACCAGCTCCTCTAAAG ACGACTTCAGCAACACCTGAACTGAATACCACCCCTCTAGAAGTCATGCT GCCAACCACCACCATCCCTAAACAACCTCCAACCCTGAAACAGCTGAAG TAAATCCAGATCATGAAGATGCAGATGGAGGTGAAGGAGAAAAACCTCT GATTCCCGGGCCCCCTGTGCTATTCCCCACAGCTATTCCAGGCACTGATC TTTTGGCCGGGAGACTCAATCGAGGCATTAACATCAATCCCATGCCTTCA GATGAGACCAATTTATGCAATGGTAAGCCAGTGGATGGACTGACTACGCT GCGCAATGGGACATTAGTTGCATTTTCGAGGTCATTATTTCTGGATGCTGA ATC
Murine Creb5	GCCTGTCCCAGGCTCTCTATCATCTCTACTCCATCTCCACAACAGACAGAG GCAGCCCATGCCGGCCTCCATGCCTGGAACCCTGCCAACCCCACCATGC CAGGATCTTCTGCCGTCTTGATGCCTATGGAGAGACAGATGTCAGTGAAC TCCAGCATCATGGGCATGCAAGGTCCAAACCTCAGCAACCCCTGTGCTTC TCCCCAAGTCCAGCCAATGCATTGAGAAGCCAAAATGAGACTGAAGGCTG CGCTGACTCACCATCCTGCCGCCATGTCGAACGGGAACATGAGCACCATC GGACACATGATGGAGATGATGGGCTCCCGGCAAGACCAGACACCCGACC ACCACCTGCACTCACACCCGCATCAGCACCAGACACTGCCGCCCCACCAC CCCTACCCACACCAGCACCAGACCCCGCACACCATCCCCACCCACAGCCT CACCACCAGCAGAACCACCCGCACCACCCTCCATTCCACCTTCACGCA

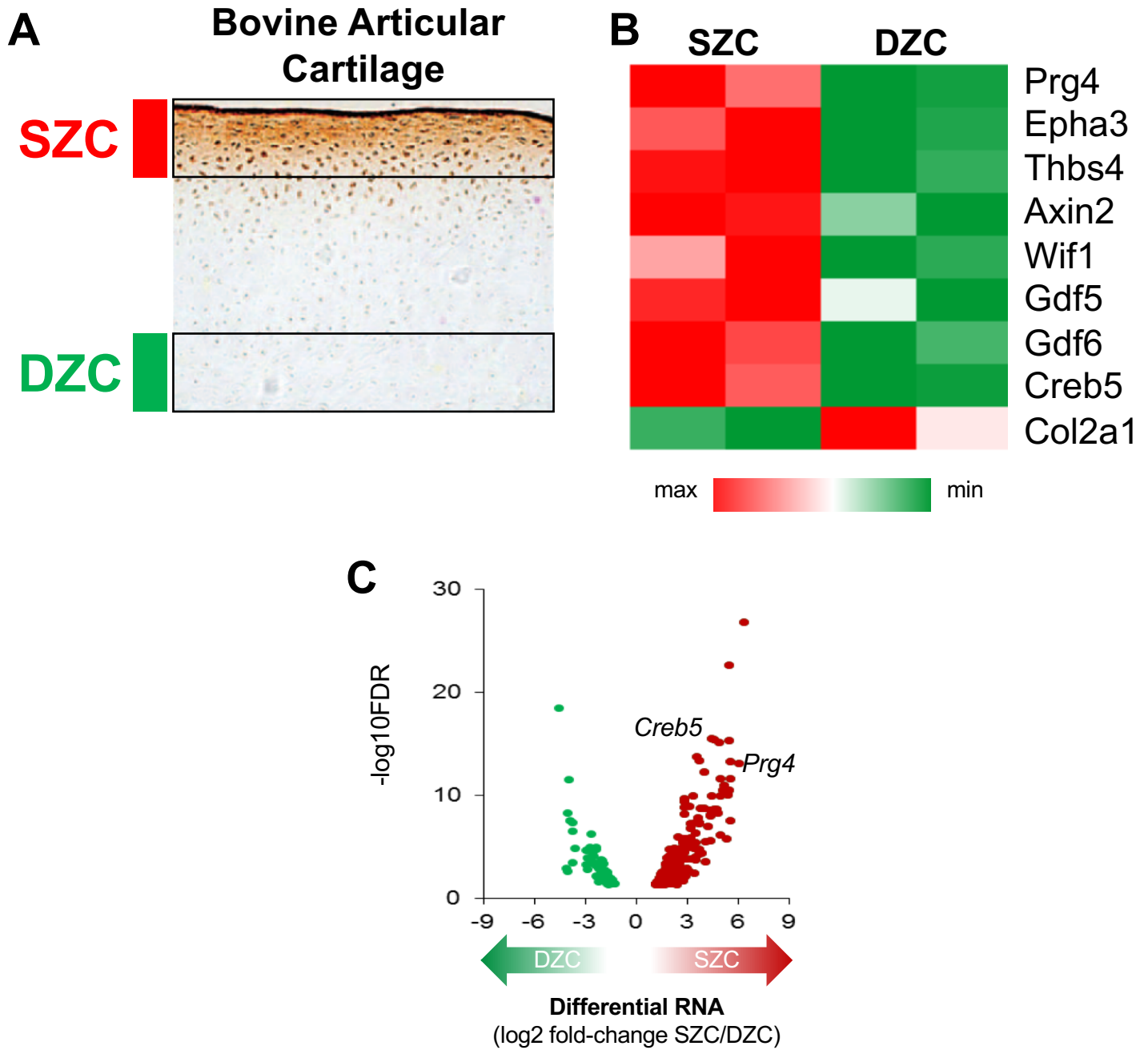
	<p>CACCCGGCGCACCACCAGACCTCGCCACACCCACCCCTGCACACCCGGCAA CCAAGCACAGGTTTCACCAGCTACACAACAGATGCAGCCAACCCAGACAA TACAACCACCCCAGCCCACAGGGGGACGCCGGCGAAGAGTGGTGGATGA GGACCCAGATGAGAGGCGGAGGAAATTTCTGGAAAGGAACCGGGCCGCC GCCACCCGCTGCAGACAGAAGAGGAAGGTCTGGGTGATGTCCTGGAAA AGAAAGCTGAAGAGCTCACCCAGACAAACATGCAGCTTCAGAATGAAGT GTCCATGTTGAAAAACGAGGTGGCCAGCTGAAGCAGTTGTTGTTAACAC ATAAAGACTGTCCGATAACAGCCATGCAGAAAGAATCCCAAGGGTATTTA AGTCCAGAGAGCAGCCCTCCTGCGAGCCCTGTGCCAGCATGCTCTCAGCA GCAAGTTATCCAACACAACACCATCACTACATCCTCATCGGTCAGCGAGG TCGTGGGGAGCTCCACCCTCAGTCAGCTTACAACCTCACAGAACAGACCTG AATCCTATTCTTTAAAAGGCATCGGTCAAACCTGGCCTTTGAGAAGAGCT GTAGCATGCCGTACATCCTTTCTCAAAGGGGCATTTTTTTTTAGAATTATCT CAGACCTGGAAGACGCCTCAGCCCTTCAAAGACTGGCTTTTCATTTTTATA GTTATTATGGAATGTTGTCTTTTATACTTAGTTATATAAGAAAAAAGGG AGATATGCAATGAATATCTATCAGCTTGGGGAGCACGTTGGTGGCTTCTCT GCAATTTTCTGGTACCAGTTTCTTGTTTATAAACGGAACCTTTCCCTGTATA TAGCCATGGTTTCATTCTTACCAGCCCAACCCTTTGCCTGGAACAATGAAT CTTGTTCAACTACAGCTTTTAGCCAAAATGAGGTATGCTTAGATGTCAAG CGAGATGGATCCACACAGTAACTGGGTGGGAAAGCTCATGATGTCATAA CTCATGTTGAGTTTGTGCTGTGATGTCACCAGAATCTCAGATAAACACAT GGGCCTTCTGAATATTTTTTCTTTGCTAGAAAAAATAAATTATGGTCC ATCCATATCCCATGAAAGCCACCAAGCATCTCAGGCCCCCTCCTCCTCTC TTTTCTACTTGTGCAGATGTCCAATATCCATCTCATTTTCTTTCCCGGA TCCCTTGTTTACTCTTTGTTTTGACTTTTTTTTTCTGTTTCTTTTCTCCCCTT TAGCTTTGCATGTAAAAAGAAAATAATGTTTAAAGAAGAGAAAAAGCAA ATCTGGAAACTGTGGACCTAGCCACAGTTTAAACCACAGCTGGAGTTCAT TCAATTTTTGCCTTTCACAAAATAGCAACCAGGAGATGTTTAAATGTGCCT GATTTAATGTTTTTAATAACCAGAGCAAATAAAAAGGTGGTTTGGTTATAG GTGAAGCACTGTTGAATGCCAGCTGTGGGGACACTAGGGAAAGGGACTT CGTAAGCTCCAACCTGTGAAAATTCAAATAAGGATGTGGGCTCTAACATCA CACCCTCGAATTACAGCTCGCTTCTATGGCCTGTCTATAATGTAAAAAATC CATGCACTATATAATAGTTCAGAAGGGCTCTGTTCACTACACAGATTACA TTGTTCAATCATCAGCTGCTAATAACCTAAGATTTATTATTATTATTTTTT TTAAGCCTATGGAACCAGCTCTGCTGTTCTGGTGGGCAAAAGCAAACCTCA CTCTGGAGCAACAGAGAGAAAGCGAGGCCAGCGTTTCTCGGGGACTCG CAGTCTGCCAGAACAGTCAGACTCCTTGGCTGCTGACCGAGTCCCATGGA GGTGGCCAGGCTGGTGCCTCATCTGAGTAGTTCTGATTTATATTTTTAG CAATGTCCACGGACTTGCCATTACAGAAAGCAGATCAAACCCAAACCAC AGTTGTGCCTCCTTGAAACAAGCCATTCTACTCTGCTGGTGTTTTACTATC GTGTTTCAAAATAATAGGGGCTAATGTTTCTCACTAGCAGTCTGGGCAT ATGCTGGTGTTCATCTCTGCCCAAATAATTACCTCCTAACCTATGTGTG TGTGTGTGTGCACATGGATGTGTGTGCCTGAGTGTGTGAGTGTGTGTGT GTGTGTGTGTGTGTGTGTGTGTGTTTATGAACAGTATAGGTTTTAAAAGA ACAGTATTTTACAAAAGCCATCACTTTTATAAGAGTTCTGTAAAGGAAGG ATGTACTTCTTCGCTCACTATAGTTTAAAAAATTTCTATTTTAGAGGAAAA AAAAAAAAAAAAAAAAAA</p>
Col2a1	<p>CCTGTCTGCTTCTTGTAACCCCGAACCCCTGAAACAACACAATCCATTG CGAACCCAAAGGACCCAAACACTTTCCAACCGCAGTCACTCCAGGATCTG CACTGAATGGCTGACCTGACCTGATGATACCCAACCGTCCCTCCCTCACA GCCCGGACTGTGCTCCCTTTCTAAGAGACCTGAACTGGGCAGACTGCAA</p>

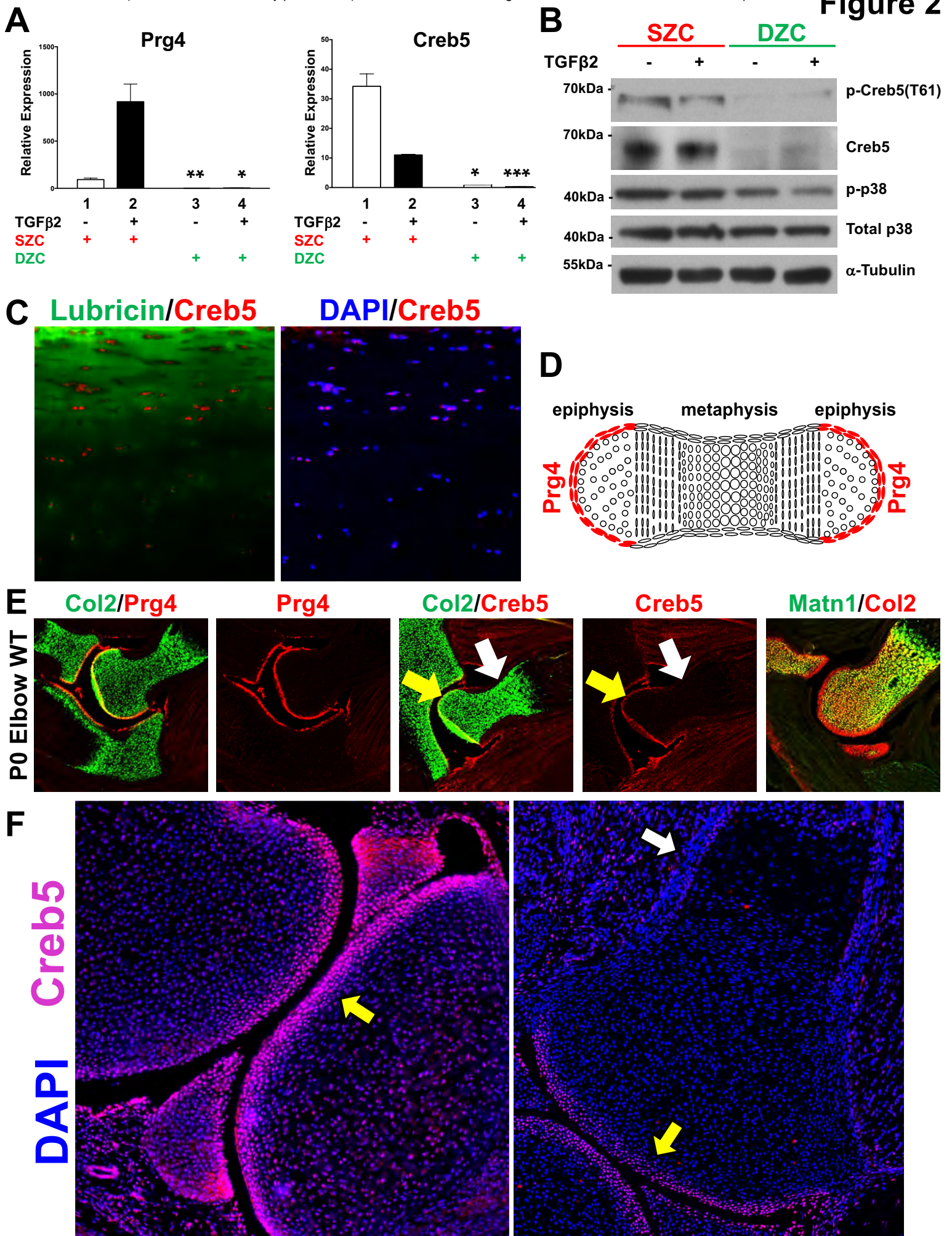
	AATAAAATCTCGGTGTTCTATTTATTTATTGTCTTCCTGTAAGACCTCTGG GTCCAGGCGGAGACAGGAACTATCTGGTGTGAGTCAGACGCCCCCGAG TGACTGTTCCAGCCCAGCCAGAAGACCCCTACAGATGCTGGGCGCAGG GACTGCGTGTCTACACAATGGTGCTATTCTGTGTCAAACACCTCTGTAT TTTTTA
Matrilin1	GGATCCAAGAGCGTGCGGCCTGAGAACTTTGAGCTGGTGAAGAAGTTCA TCAACCAGATTGTGGACACGTTAGATGTGTTCGGACAGGCTAGCCCAGGT GGGGCTGGTGCAGTACTCCAGCTCCATTCGCCAGGAGTTCCCACTCGGCC GCTTCCACACCAAGAAGGACATTAAGGCCGCGGTGCGGAACATGTCTAC ATGGAGAAAGGCACCATGACTGGCGCCGCCTTGAAGTATCTCATAGATAA TTCTTTCACTGTGTCCAGCGGGCAAGGCCTGGAGCCCAGAAGGTGGGC ATCGTCTTACCCGATGGCCGGAGCCAGGACTACATTAATGACGCTGCCAG GAAGGCCAAGGACCTTGGCTTTAAGATGTTTGCGGTGGGCGTGGGCAAT GCTGTGGAGGAAGAGCTGAGGGAGATCGCTTCCGAGCCCGTGGCAGACC ACTACTTTTACACAGCTGACTTCAAGACCATCAACCAGATTGGCAAGAAG CTGCAGAAACAAATCTGTGTGGAGGAAGACCCCTGTGCTTGTGAGTCCAT ACTGAAATTTGAGGCCAAGGTGGAGGGTCTGCTGCAGGCCCTGACCAGG AAGCTGGAAGCTGTGAGCGGGCGGCTGGCTGTCCTGGAGAACAGAATCA TCTAA

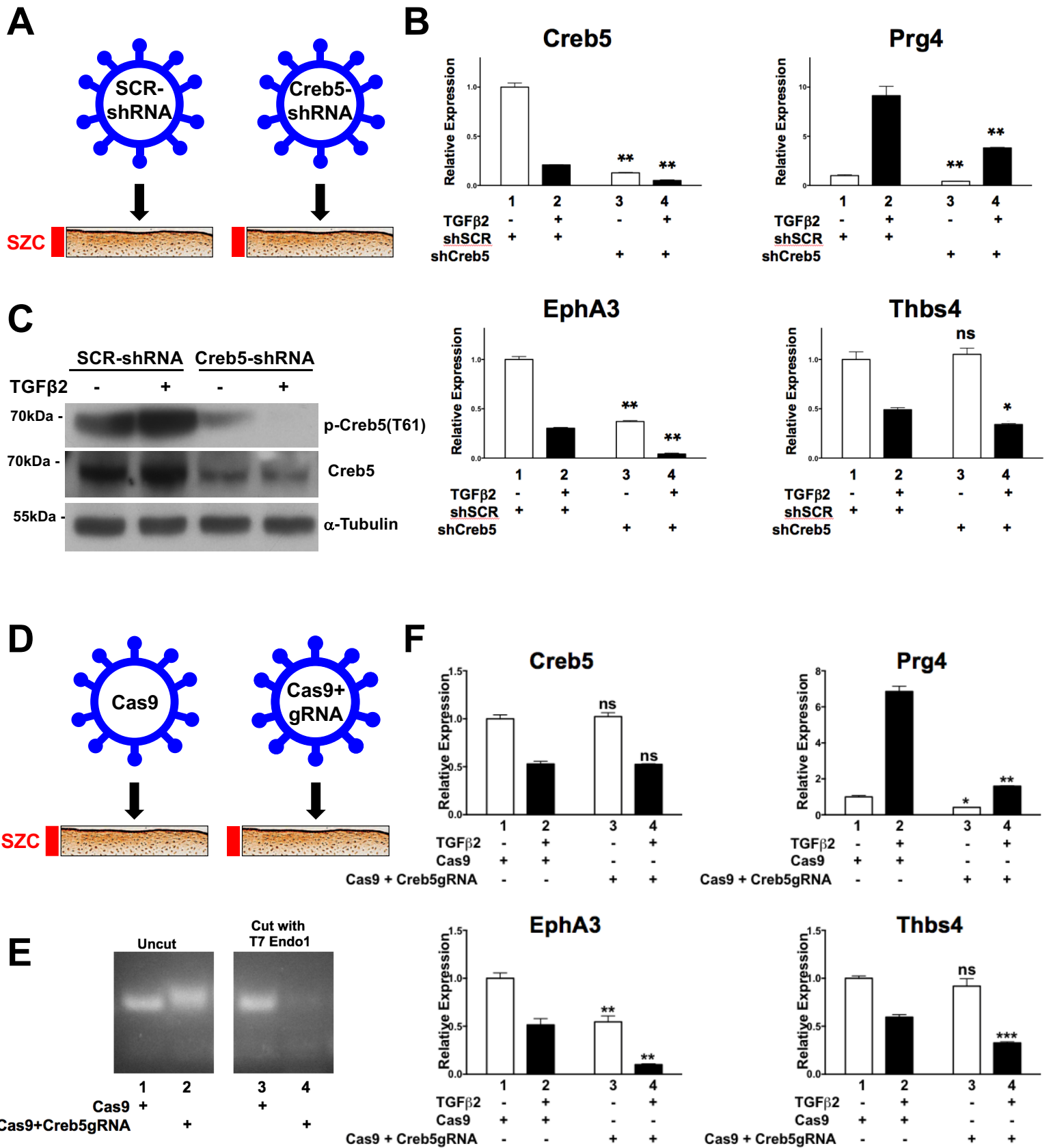
Supplementary Table 11: PCR primers for human *PRG4* and *GAPDH*

Gene	Forward	Reverse
<i>PRG4</i>	TGTGACTGCGACGCCCAATGTA	GGTTTGAGATGCTCCTGAAGGTG
<i>GAPDH</i>	GTCTCCTCTGACTTCAACAGCG	ACCACCCTGTTGCTGTAGCCAA

Figure 1







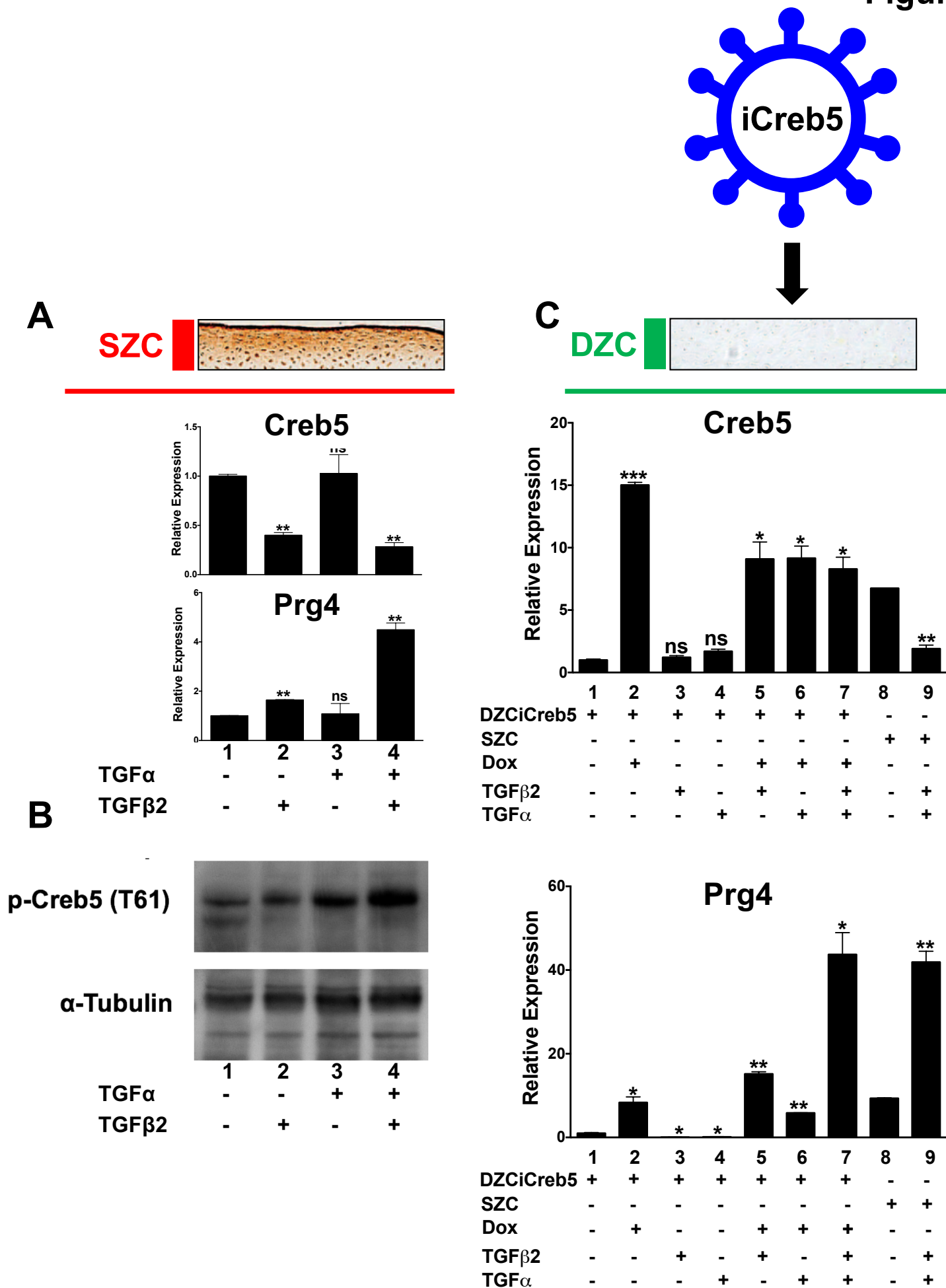
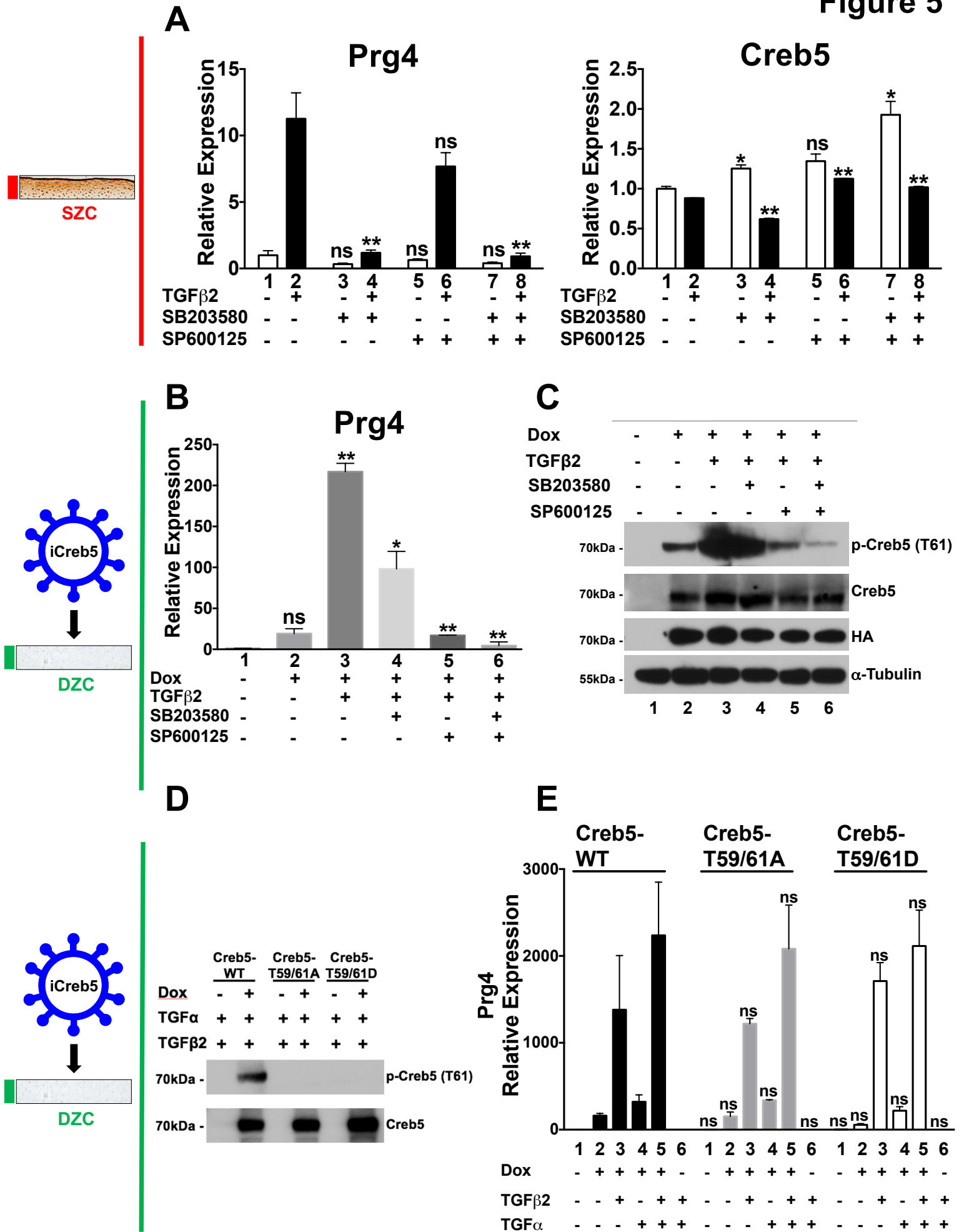









Figure 5



A Binding motifs enriched in Superficial Zone Specific ATAC-Seq peaks

Rank	Motif	P-value	log P-value	% of Targets	% of Background	STD(Bg STD)	Potential binding site for:
1		1e-53	-1.225e+02	18.19%	4.38%	55.9bp (58.7bp)	Creb5/Creb5 or Creb5/Jun
2		1e-40	-9.414e+01	30.54%	13.27%	53.7bp (63.5bp)	NFI
3		1e-34	-8.032e+01	19.07%	6.66%	52.8bp (57.9bp)	Creb5/Creb5 or Creb5/Jun
4		1e-32	-7.491e+01	33.52%	17.07%	56.5bp (61.1bp)	NFAT
5		1e-16	-3.889e+01	3.20%	0.38%	55.7bp (69.2bp)	TBX

B Binding motifs enriched in Deep Zone Specific ATAC-Seq peaks

Rank	Motif	P-value	log P-value	% of Targets	% of Background	STD(Bg STD)	Potential binding site for:
1		1e-51	-1.178e+02	24.22%	7.29%	52.0bp (62.6bp)	TEAD
2		1e-45	-1.057e+02	23.49%	7.47%	53.4bp (62.7bp)	RUNX

C

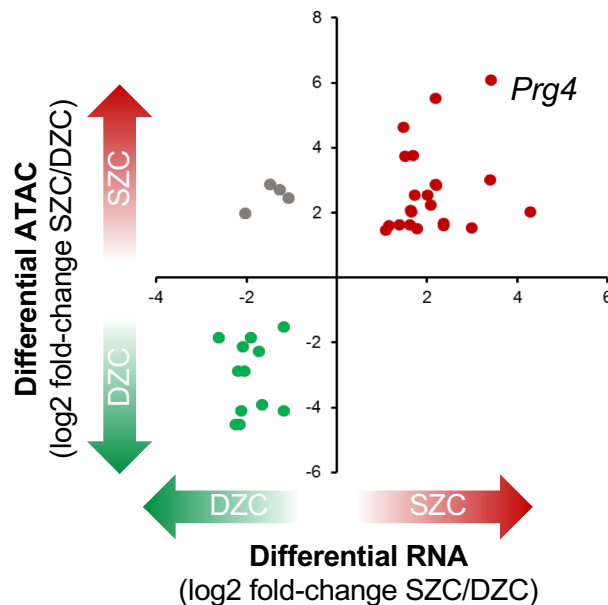
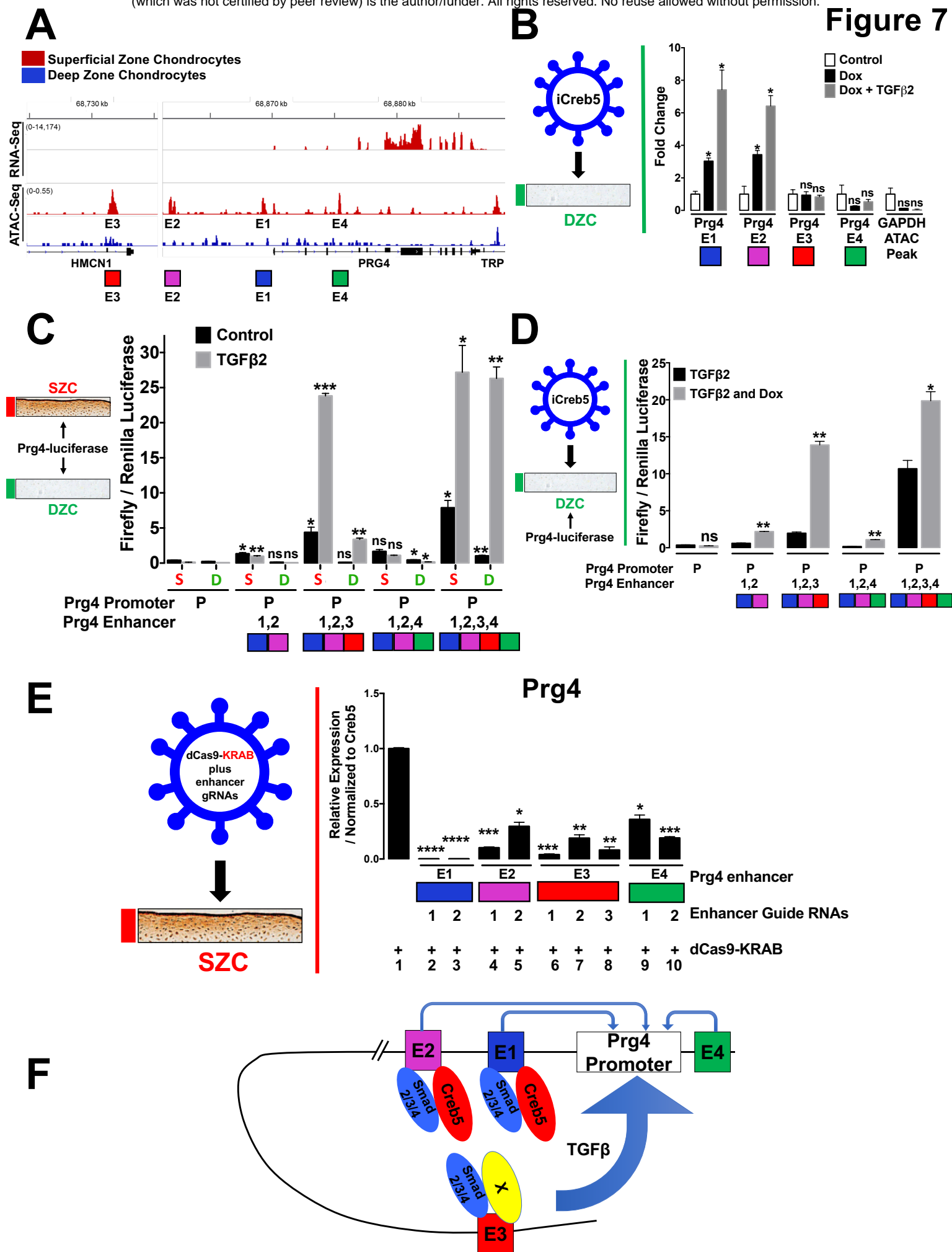
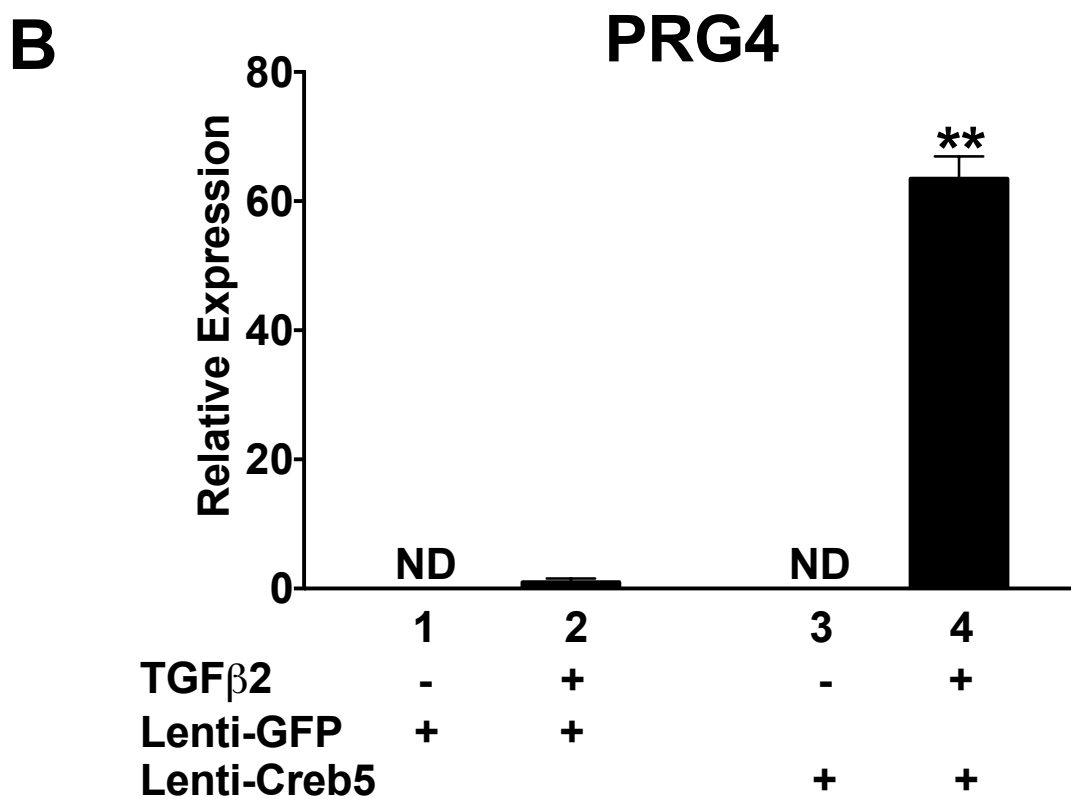
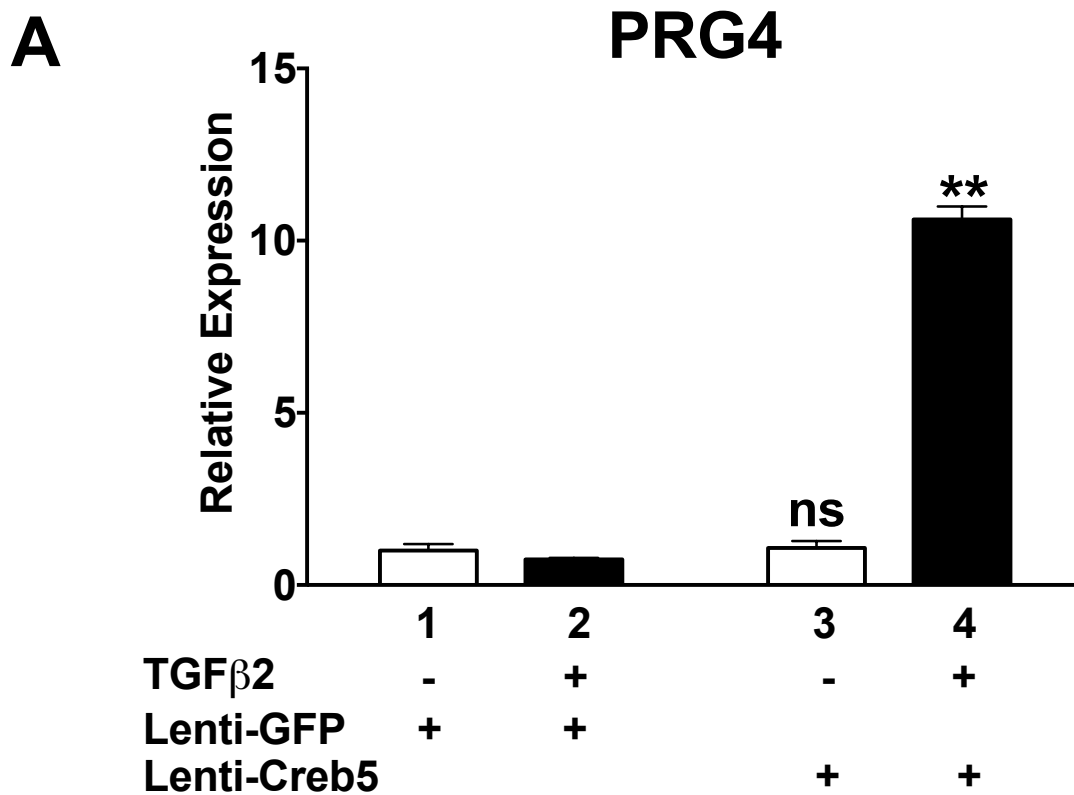


Figure 7

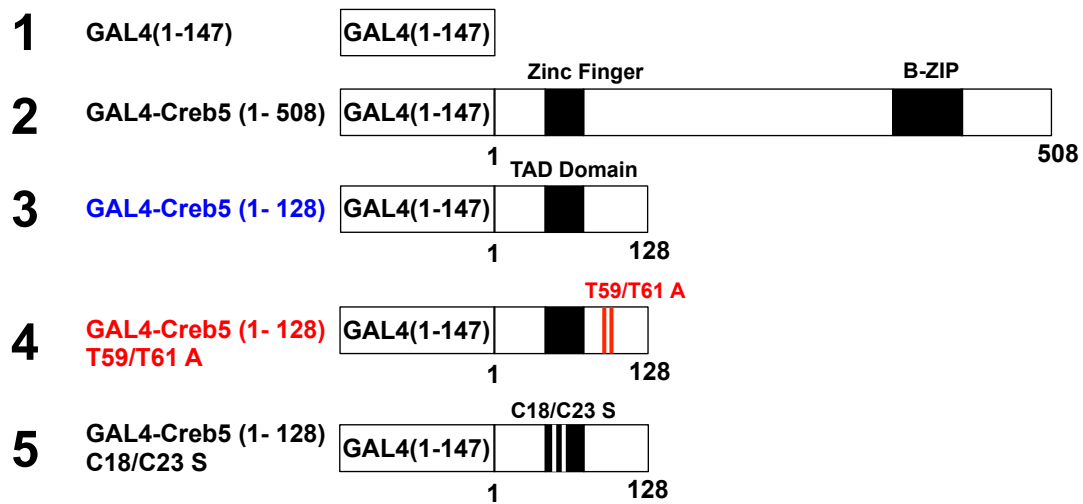


Supplementary Figure 1

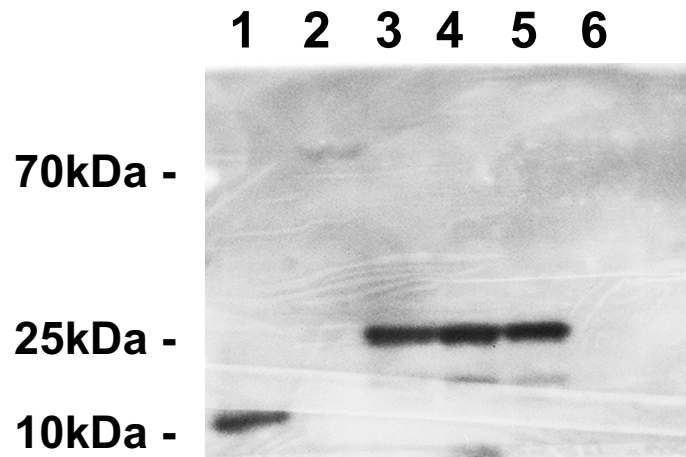


Supplementary Figure 2

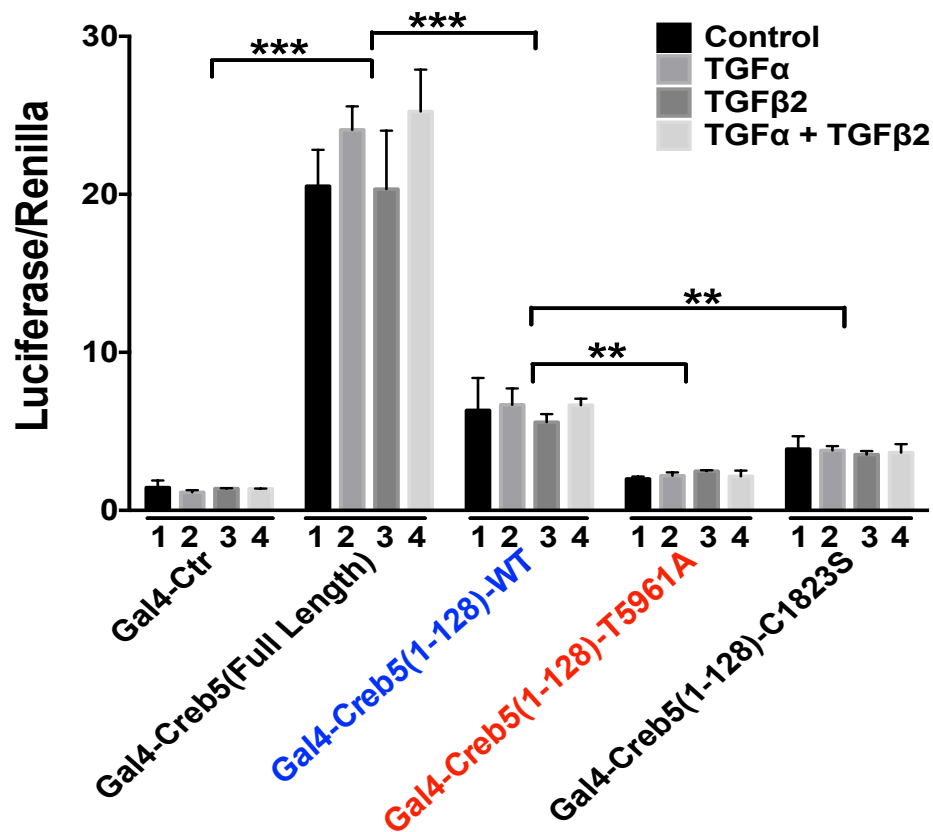
A



B



C



Supplementary Figure 3

